AD

161 494

ENGINEERING REPORT

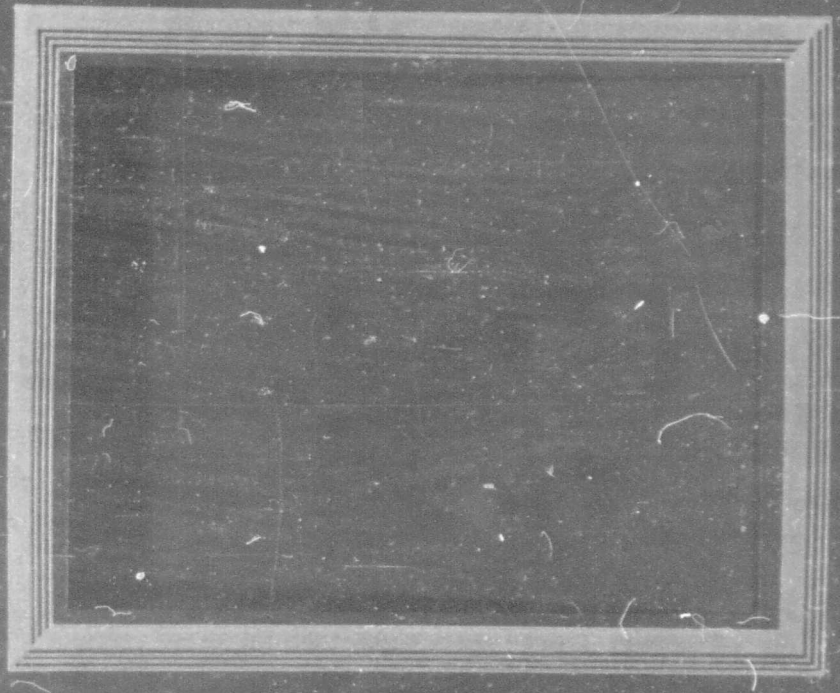

HAMILTON STANDARD

7-12

Hamilton Standard Report No. HS-1829

GENERALIZED PERFORMANCE OF CONVENTIONAL PROPELLERS FOR VTOL-STOL AIRCRAFT

Submitted by
Hamilton Standard
Division of United Aircraft Corporation
Windsor Locks, Connecticut

Contract No. Nonr 2203(00)
Amendment No. 1

Written by: Albert M. Stuntman — Aerodynamics Engineer

Approved by: George Rosen — Chief of Analysis

D. G. Richards — Chief of Technical Staff

March 31, 1958

Bibliographical Control Sheet

1. Originating agency, and/or monitoring agency:

   O. A.: Hamilton Standard, Windsor Locks, Connecticut
   M. A.: Office of Naval Research, Air Branch (Code 461), Washington 25, D. C.

2. Originating agency report number

   O. A.: Hamilton Standard Report No. HS-1829

3. Title and Classification of title

   "Generalized Performance of Conventional Propellers for VTOL-STOL Aircraft" - (Unclassified)

4. Personal Authors: Shenkman, A. M.

5. Date of Report: March 31, 1958

6. Pages: 58

7. Illustrative Material: Thirty-three pages (graphs)

8. Prepared for Contract No: Nonr 2203(00)

9. Security Classification: Unclassified

10. Abstract:

A report on the generalized performance of conventional aircraft propellers operating in a skewed flow field representative of propeller operation on VTOL and STOL aircraft.

TABLE OF CONTENTS

SUMMARY

This report provides a generalized performance presentation, including normal force and shaft moments, for conventional aircraft propellers operating in a skewed flow field representative of propeller operation on VTOL and STOL aircraft. This report also includes generalized propeller performance for steady state operation of propellers in an unskewed flow field. The estimated performance data has been based on the Hamilton Standard form of strip analysis method of propeller performance calculation.

This report is submitted in accordance with Section D of Amendment No. 1 dated 21 May 1957 to Contract No. Nonr 2203(00). This fulfills the contractual requirement of Phase I of the subject contract.

The contractual requirements for airfoil testing under Phase II and Phase III of the subject contract are covered by Hamilton Standard Reports HS-1829A and HS-1829B respectively.

INTRODUCTION

In view of the increasing interest in vertical rising and short take-off aircraft, considerable thought is being given to the kind of propulsive system required for these types of aircraft. In order to provide the extremely large thrusts required to accomplish short take-off, many radical and complex propulsive systems are being considered. Some of these devices being studied are modifications of the conventional propeller, including boundary layer control by blowing or sucking through slots along the blade, large turning flaps, and shrouds. In addition, slip-stream turning devices on the fixed wing behind the propeller, and rotatable wings are being investigated. Although it may be established eventually that one or more of these radical systems may be required, the aircraft would be greatly simplified by utilizing a conventional propeller. Thus, it would appear that the suitability of conventional propellers for short take-off and vertical rising aircraft needs to be established.

While the applicability of these propellers to the subject aircraft will eventually need to be studied from a structural standpoint, an indication of the performance attainable from propellers designed to provide large thrusts at low airspeeds is required at an early date. Moreover, the effect on airplane stability and performance of the normal forces and shaft moments produced by conventional propellers inclined to the airstream needs to be examined. Thus, in addition to the thrust and torque performance, an indication of the magnitude of the normal forces and shaft moments for the propeller operating range is required. Although the NACA has conducted tests on model propellers inclined to the airstream and a limited amount of data from other sources is available, there was a need for a generalized set of data, in a form suitable for direct analysis of VTOL/STOL propeller performance.

This report covers the results of an analytical study to derive estimated thrust and torque charts and estimated normal force and shaft moment charts for conventional propellers designed to produce large thrusts at low airspeeds. The foregoing is aimed at providing a generalized propeller performance and force and moment presentation for use in evaluating conventional propulsive systems for short take-off and vertical rising aircraft.

DISCUSSION

When the thrust axis of a propeller disc is inclined with respect to the forward free-stream velocity, the propeller undergoes a cyclic variation in resultant velocity and inflow angle once per revolution and a corresponding variation in aerodynamic loading. In view of the unsteady nature of the flow, the problem of calculating the force and moment characteristics is a most complicated one. Inasmuch as there is no adequate three-dimensional unsteady aerodynamic theory covering propellers operating under inclined airflow conditions, it was necessary to investigate several methods of performance analysis to see which one would give best results with available test data. This included the consideration of the effects of two-dimensional unsteady aerodynamics as well as steady state incompressible aerodynamics. A literature survey of two-dimensional oscillating airfoil data revealed a negligible amount of experimental data. (Ref. 1,2) The theoretical data are based on two-dimensional flat plate potential flow which does not take into account the effects of compressibility shock, airfoil stall, and drag characteristics associated with actual airfoils. (Ref. 3, 4, 5, 6) However, since the two-dimensional effect of unsteady flow may well be more predominant than the induced effects due to the three-dimensional flow, it was felt that an analysis utilizing airfoil data based on two-dimensional unsteady aerodynamics should be conducted.

When attempts were made to incorporate the effects of unsteady aerodynamics based on the above considerations, the range of data coverage was limited to conditions where the airfoil was operating on the straight line portion of the lift curve. The results of this analysis showed good agreement with test data. However, in the general case, the theoretical approach does not hold, since the blade sections would be operating either in positive stall or negative stall, or both, and the viscous (drag) effects would be most consequential.

In view of the limitations to the application of unsteady aerodynamics, as shown above, a comprehensive analysis of steady state incompressible aerodynamics was made. Accordingly, although it does not offer a rigorous solution, steady state incompressible aerodynamics has been chosen as the method of computation, since it showed very good agreement with test data over the complete range of operation necessary for this analysis.

Considering a propeller in inclined flow, the forces and moments considered will now be defined. The principal force and moment vectors generated by the inclined propeller are the thrust, torque, normal force, and a bending moment applied to the propeller shaft. They are shown in Figure 1. The thrust axis is perpendicular to the plane of the propeller disc. The normal force acts perpendicular to the thrust axis, is in the plane of the propeller disc, and is essentially in the direction of inclination, except for a small component in a direction normal to the inclination and in the plane of the propeller. The latter comes about because of the phase shift due to the aerodynamic lag associated with the unsteady flow phenomena. However, this component of the normal force is very small in magnitude and may, therefore, be considered insignificant in the range of operation considered. For purposes of this study, the normal force considered will be defined as one acting in the direction of inclination. Similarly, the major bending moment on the shaft acts about an axis in the plane of the propeller disc and essentially

DISCUSSION (Continued)

in the direction of inclination. There is a small component of the moment which acts about an axis in the plane of the propeller disc but perpendicular to the direction of inclination. This component of the moment is due to the lag effects and is also small enough to be neglected in this study.

Because steady state incompressible aerodynamics does not include lag effects, the minor forces and moments calculate to zero. Although this is a limitation of steady state incompressible aerodynamics, this is not a serious situation, since the test data shows these forces and moments are practically zero in the range of operation considered for this analysis.

The study has shown that, for the advance ratio and power range applicable to the transition range of VTOL-STOL aircraft, the variation of resulting blade forces on the skewed propeller is essentially sinusoidal. This was established by first considering twelve azimuth positions at thirty degree intervals. When the various forces and moments were summed up at any given instant of time, it was found that the results were identical to the summation at any other instant of time. For a four-bladed propeller, as shown in the illustration (Fig. 2), at azimuth position, ωt, equal to zero, blades A and C are operated exactly as in a steady state, unskewed condition, whereas blade B is full advancing and blade D is full retreating. At any given azimuth position (or time), ωt, the summation of the forces (regardless of which force it is, either on a section basis or integrated values), is constant. Thus, for a four-bladed propeller, it is only necessary to consider two azimuth positions, i.e., blade A at 45° (same analysis as blade B at 135°) and blade C at 225° (same analysis as blade D at 315°).

A similar analogy holds for a three-bladed propeller. However, it was found necessary to analyze three azimuth positions, none of which involved a full-advancing or a full-retreating blade so as to keep the angles of attack as low as possible. A two-bladed propeller does not have steady loads, and, therefore, was not considered in this study.

Having established a method of computation, the existing Hamilton Standard two-dimensional lift and drag data had to be extended beyond the normal range of a propeller's steady state operating conditions to cover the extreme variation of angle-of-attack experienced by the blade airfoils on propellers operating at large inflow angles. This was accomplished by utilizing the results of the United Aircraft Corporation Research Department wind-tunnel data associated with this proposal (Phases II and III). (Ref. 7, 8). An evaluation of the flapped airfoil data indicated that the use of flaps for the type of application considered in this report offers no advantage over uniform camber. Therefore, separate analysis of flapped airfoils was not undertaken. A thorough review of other existing United Aircraft Corporation Research Department two-dimensional airfoil data (Ref. 9, 10) was also accomplished along with NACA data (Ref. 11) in order to obtain the most reliable definition of the lift and drag data in the normal operating range of a propeller. Thus, for purposes of the subject study, the previously available two-dimensional airfoil data for the family of NACA 16-Series airfoils have been fully revised and extended to cover thickness ratios up to 35 per cent, a design lift coefficient range from zero to 1.0 and an angle-of-attack range from -90° to +90°.

DISCUSSION (Continued)

A strip analysis program on the IBM 704 computer was then modified to include the revised airfoil data and provisions for obtaining propeller performance and force and moment data at inflow angles from zero to 70°. As the inflowangle approaches 90°, a condition develops with extreme amplitudes of blade section angle-of-attack and with the airfoils in the inboard portion of the blade actually experiencing negative velocities or reverse flow at certain azimuth positions. Due to the fact that wind tunnel testing techniques have not been established for obtaining reliable airfoil characteristics under these extreme conditions, this poses a definite limitation on the range of angles of inclination that can be analyzed by a purely analytical method. This study has indicated that, with the range of airfoil data available, this limitation on angle of inclination is approximately 70°, and, accordingly, the method of analysis presented herein should not be applied beyond this point. Since it appears that the definition of performance of propellers with inflow angles between 70 and 90 degrees cannot readily be defined by purely analytical means, this region must be established by wind tunnel testing.

Many check calculations were run off to compare with both hand calculations and NACA wind tunnel data. These calculations indicated good agreement with test results (Ref. 12) in the lightly loaded cases covered in this report. A check with wake survey data for inflow angles up to 15° showed very good agreement in checking out blade section loadings. (Ref. 13)

A family of propeller configurations was then selected to examine the effect of activity factor, side force factor, integrated design C_L, and number of blades. These shape variables are as follows for propellers with blades of rectangular planform and pitch distribution selected as best for cruise:

Number of Blades	3 and 4
Activity Factor	100, 140, 180
Side Force Factor	95, 133, 171
Integrated Design C_L	0.300, 0.500, 0.700

The four-way, 140 activity factor and 0.500 integrated design C_L, 133 side force factor blade was chosen as the basic blade for the basic set of plots.

After thoroughly examining the results obtained for the basic blade through the complete inflow angle range (at ten degree intervals) and also comparing the basic blade (0.500 integrated design C_L) with blades similar in all respects except for camber, a method of presentation successfully used by the Hamilton Standard Aerodynamics Department for generalized propeller performance was chosen for the thrust and the torque. This includes base charts for both the thrust and torque coefficients as a function of effective advance ratio and blade angle at the three-quarter radius with appropriate correction for activity factor, number of blades and integrated design C_L.

It must be noted that the range of thrust and torque coefficients included in the base plots extend to negative values. This is not intended

DISCUSSION (Continued)

as a basis of predicting negative thrust or windmilling performance; but, since the camber correction and the method of solving for the coefficients at an inflow angle is an additive function, it is necessary to include these negative values to predict the performance of large size (highly cambered, large activity factor) blades. The effective advance ratio, J' (equal to the advance ratio times the cosine of the yaw angle) has been chosen as a parameter since it has been successfully used by the NACA (Ref. 12) and gives the best correlation of the data. Generalization of the thrust and torque coefficients through the inflow angle range has been accomplished by adding to the base chart (for zero inflow angle), a parameter that is both a function of effective advance ratio and inflow angle, and by providing correction factors for number of blades, activity factor and camber.

After carefully reviewing the normal force coefficient and shaft moment coefficient, it was noted that both coefficients are proportional to the tangent of the inflow angle at a constant blade angle and effective advance ratio basis. Number of blades and camber corrections are applied in a similar manner as for the torque and thrust. However, although the moment coefficient is a function of activity factor, it was found that the normal force coefficient is a function of side force factor.

The base charts and correction factor charts resulting from the subject study together with a detailed procedure for their use is presented in Appendix A. In addition, Appendix B presents a set of efficiency charts for several representative propellers, since these provide an alternate and quicker method of propeller analysis for unskewed operation. A generalized compressibility correction for use with unskewed conditions is included in Appendix C. The compressibility correction factor, Ft, may be applied directly to either a thrust or an efficiency, depending on whether Appendix A or Appendix B is utilized. No compressibility correction was derived for skewed propeller operation due to the difficulty of defining an average compressibility effect when the blades are experiencing periodically oscillating air loads. However, this does not represent any particular limitation on the utility of these charts since skewed propeller operation during STOL/VTOL aircraft transition will be accomplished at very low air speeds. Under such conditions, no appreciable compressibility effects will occur when the propeller is oriented at sizeable angles of inclination with the air stream direction. Sample calculations are included with each Appendix.

CONCLUSION

The results of this study have permitted the development of a form of generalized performance presentation for both skewed and unskewed propellers which is self contained and readily applicable to the analysis of the performance of STOL and VTOL propellers.

In order to accomplish the propeller performance generalization, approximately 5,000 strip analysis calculations were run off on the I.B.M. 704 computer. In the range of light power loadings, which is most representative of VTOL/STOL propeller operation, the generalization was found to be quite good. Actually, the generalization of the torque is good through the complete range considered, but the accuracy of the thrust, normal force and moment generalization deteriorates somewhat in the range of high power loadings where the blade airfoils become stalled. However, the maximum errors encountered in the stall regions were generally less than ten per cent, and the method can still be relied on to provide proper trends of performance with variation of the pertinent parameters.

REFERENCES

1. NACA Subcommittee on Vibration and Flutter: Confidential Report NACA RM56I12, October, 1956.

2. Smith, Maurice H. (compiled by): Bibliography on VTOL and STOL Aircraft. Literature Search No. 12. James Forrestal Research Center, Princeton University, January, 1957.

3. Lemnios, Andrew A.: Progress Report on Unsteady Aerodynamics of 1-P Loading of Propellers. United Aircraft Corporation Research Department Report M-0952-1, March 14, 1957.

4. Loewy, Robert G.: Tables of Two-Dimensional Oscillating Airfoil Coefficients for Rotary Wings. Cornell Aeronautical Laboratory Report No. 77. December, 1955.

5. Loewy, Robert G.: A Two-Dimensional Approximation to the Unsteady Aerodynamics of Rotary Wings. Cornell Aeronautical Laboratory Report No. 75. October, 1955.

6. Rogallo, Vernon L., Paul F. Yaggy, and John L. McCloud, III: An Analysis of Once-Per-Revolution Oscillating Aerodynamic Thrust Loads on Single-Rotation Propellers on Tractor Airplanes at Zero Yaw. NACA Report 1295, 1956.

7. Grose, Ronald M.: Tests of Two-Dimensional NACA 16-Series Airfoils Having High Camber and Flaps. Hamilton Standard Report No. 1829A (United Aircraft Corporation Research Department Report R-1146-1) December 12, 1957.

8. Clark, James W.: Second Series Tests of Two-Dimensional NACA 16-Series Airfoils Having High Camber and Flaps. Hamilton Standard Report No. 1829B (United Aircraft Corporation Research Department Report R-1146-2) March 6, 1958.

9. Manoni, L. R., and E. C. Breed: Confidential Report. Hamilton Standard Report No. HS-1282 (United Aircraft Corporation Research Department Report No. R-2574-10), 1955.

10. Flynn, G. A., and R. Gamage: Report on the Aerodynamic Characteristics of NACA 16-Series Airfoils. United Aircraft Corporation Research Department Report R-5071-3. January 24, 1947.

11. Lindsey, W. F., D. B. Stevenson and Bernard N. Daley: Aerodynamic Characteristics of 24 NACA 16-Series Airfoils at Mach Numbers Between 0.3 and 0.8. NACA Technical Note 1546, 1948.

12. McLemore, H. Clyde, and Michael D. Cannon: Aerodynamic Investigation of a Four-Blade Propeller Operating Through an Angle-of-Attack Range From 0° to 180°. NACA Technical Note 3229, June, 1954.

13. Russell, J. G.: Wake Survey and Strain-Gauge Measurements on an Inclined Propeller in the R.A.E. 24-Foot Tunnel. Part 1: Wake Survey. Great Britain Aeronautical Research Council Current Paper No. 117, 1953.

COEFFICIENTS AND SYMBOLS

T	-	Propeller thrust, lb.
F_N	-	Propeller normal force, lb.
Q	-	Propeller torque, ft.-lb.
M	-	Propeller shaft moment, ft.-lb.
C_T	-	Thrust coefficient, $T/\rho n^2D^4$
Tc	-	Thrust coefficients, $(C_T) \times (1/J')^2$
C_N	-	Normal force coefficient, $F_N/\rho n^2D^4$
N_C	-	Normal force coefficient, $(C_N)(1/J')^2$
C_Q	-	Torque coefficient, $Q/\rho n^2D^5$
Cp	-	Power coefficient, $2\pi C_Q$
Qc	-	Torque coefficient, $(C_Q)(1/J')^2$
C_M	-	Shaft moment coefficient, $M/\rho n^2D^5$
Mc	-	Shaft moment coefficient, $(C_M)(1/J')^2$
A.F.	-	Blade activity factor, $\frac{100,000}{16}\int_{.15}^{1.0}\left(\frac{b}{D}\right)(x^3)\,dx$
b	-	Blade section width, feet
B	-	Number of blades
BHP	-	Shaft-brake horsepower
C_{L_D}	-	Blade section design lift coefficient
C_{Li}	-	Integrated design C_L, $4\int_{.15}^{1.0} C_{L_D}(x^3)dx$
D	-	Propeller installed diameter, feet
Fc	-	Ratio of the square root of the absolute temperature, T_0/T
Ft	-	Compressibility correction factor
G.R.	-	Gear ratio, propeller speed/engine speed
J	-	Propeller advance ratio based on stream-wise component of velocity, v/nD
J'	-	Effective propeller advance ratio based on velocity component normal to propeller disc, J cosine ψ

COEFFICIENTS AND SYMBOLS (Continued)

K_T	-	Inflow parameter for thrust, a function of J'
K_Q	-	Inflow parameter for torque, a function of J'
M_{AF}	-	Activity factor correction to moment coefficient
n	-	Propeller speed, revolutions per second
N	-	Propeller speed, revolutions per minute
Ne	-	Engine speed, revolutions per minute
N_{SFF}	-	Side force factor correction to normal force coefficient
Q_{AF}	-	Activity factor correction for torque coefficient
r	-	Radius at blade element, feet
R	-	Blade radius at propeller tip, feet
S_{FF}	-	Side force factor, $\frac{100,000}{\Sigma Z} \int_{.20}^{1.0} \frac{b}{D} \sin \theta \, dx$
T_{AF}	-	Activity factor correction for thrust coefficient
v	-	Inflow velocity, feet per second
V_K	-	Inflow velocity, knots
x	-	Fraction of propeller tip radius, r/R
η	-	Propeller efficiency, $J\left(\frac{C_T}{C_P}\right)$
θ	-	Propeller blade angle, degrees
ρ	-	Mass density of air, slugs/cubic foot
ρ_c/ρ	-	Density ratio
ψ	-	Inflow angle, also referred to as angle of inclination
ψ_T	-	Inflow parameter for thrust, a function of ψ
ψ_Q	-	Inflow parameter for torque, a function of ψ
Δ coefficient	-	Camber correction factor

COEFFICIENTS AND SYMBOLS (Continued)

Postscripts

'	- Refers to effective coefficients (corrected to the basic configuration assumed for the base charts)
"	- Refers to effective coefficient (corrected for four blades and 140 activity factor or 133 side force factor)

Subscripts

Ψ	- Denotes coefficient at proper inflow angle
3/4	- Denotes 3/4 blade radius

LIST OF FIGURES

As a matter of convenience, the figures are included in the text or the appendices, depending on where they are used.

TEXT

APPENDIX A

LIST OF FIGURES (Continued)

HAMILTON STANDARD

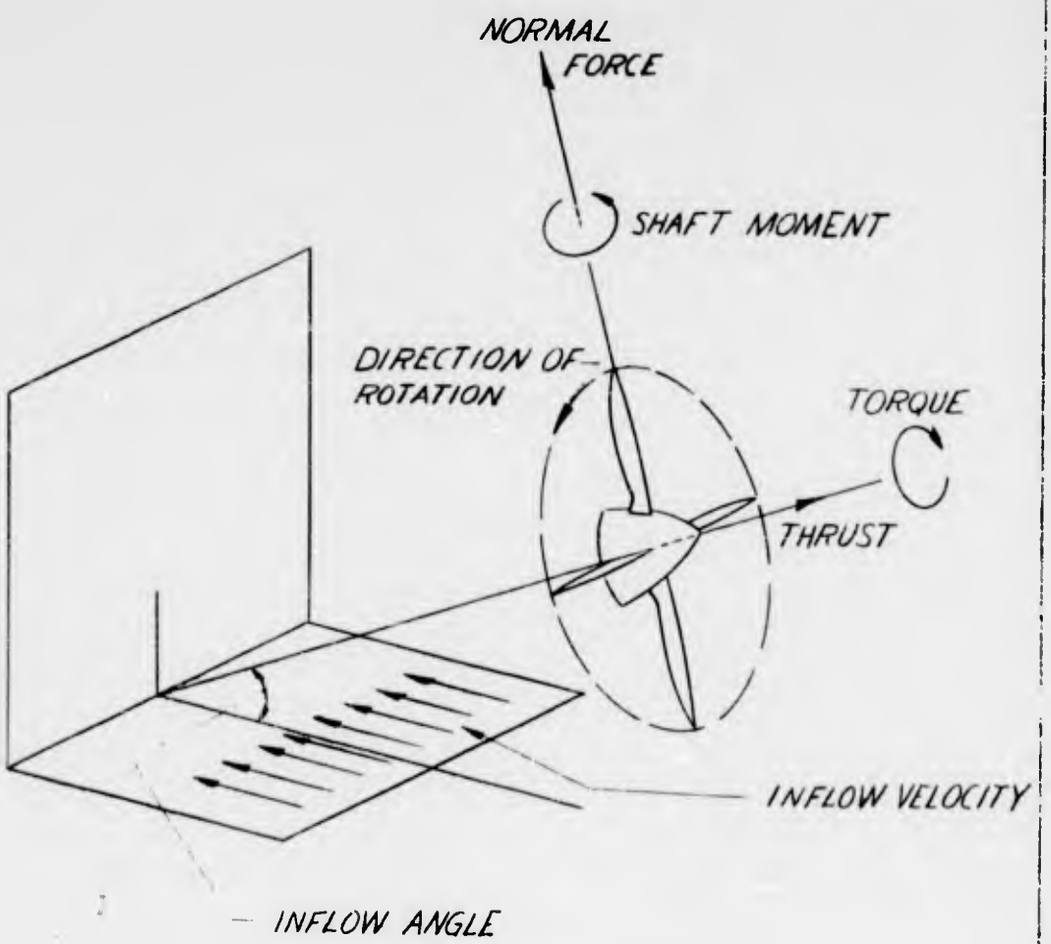

DEFINITION OF PRINCIPAL FORCE AND MOMENT VECTORS

GENERATED BY AN INCLINED PROPELLER

HAMILTON STANDARD

THE VELOCITY VECTOR DIAGRAM FOR A BLADE SECTION AT MAXIMUM AND MINIMUM ANGLES OF ATTACK

(THIS DEFINES THE STEADY-STATE, ADVANCING, AND RETREATING BLADES.)

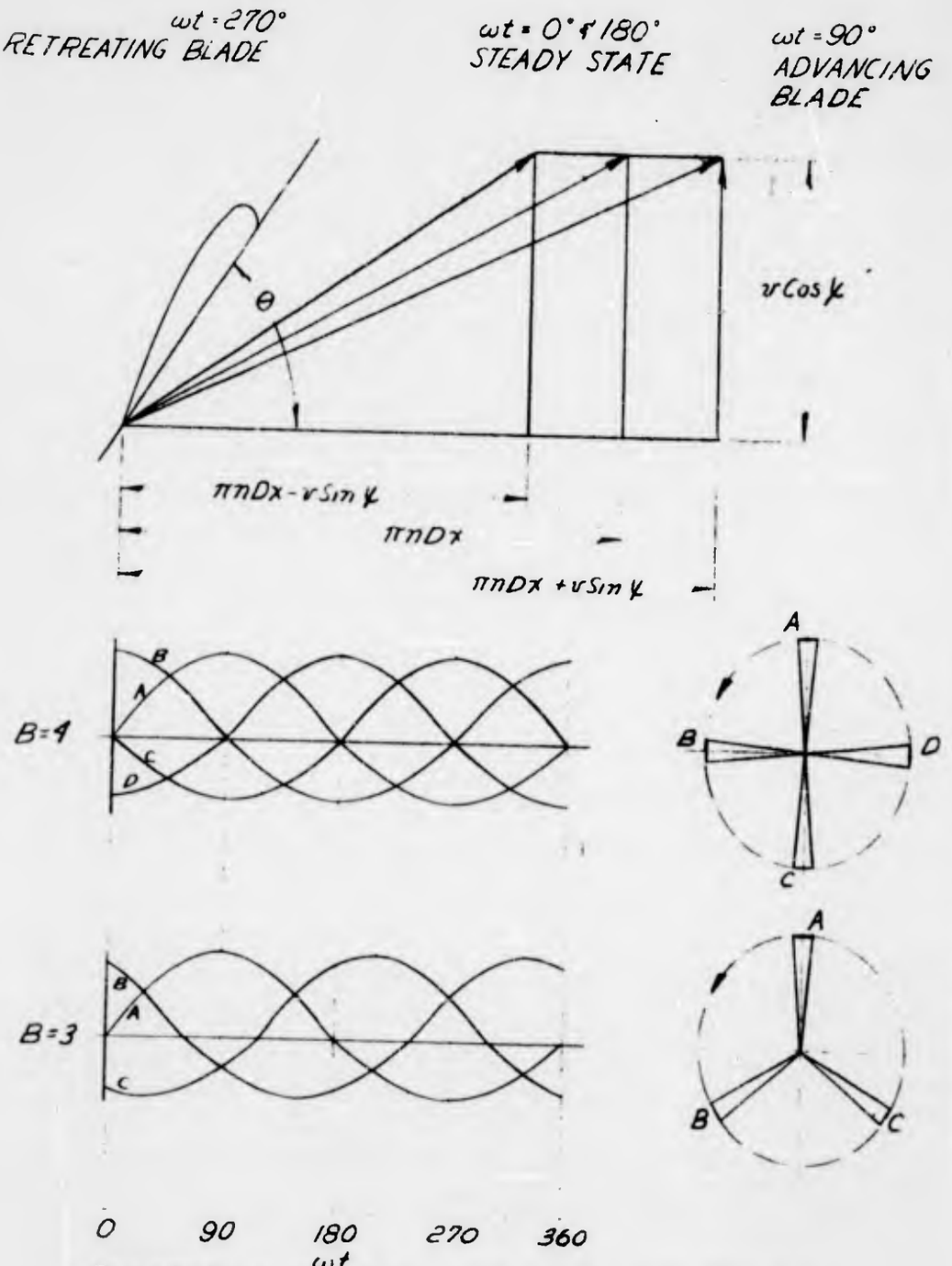

Representative Form of Calculated Blade Loading Variations.

APPENDIX A

PERFORMANCE CALCULATION PROCEDURE

The following presents the method of calculating the performance, normal force and shaft moment which was developed as described in the discussion. Used in conjunction with the symbols and definitions and the following procedure, all operations are self-explanatory. Given the airplane flight and engine conditions and the propeller blade characteristics, the procedure as outlined on the sample computation sheets is as follows:

(A) From known data, complete top of the first computation sheet (which follows). Identify airplane, engine, gear ratio, number of blades (or hub), blade designation, diameter, activity factor, side force factor and integrated design C_L.

(B) Determine items numbered 1 to 5 inclusive from the airplane flight and engine conditions which have been selected for analysis, as explained below:

Item Number

1	Attitude - Identifying flight condition
2	BHP - Engine shaft - brake horsepower
3	Ne - Engine speed (revolutions per minute)
4	Vk - Airplane forward velocity or inflow velocity (knots)
5	Altitude - Height of operation (feet)

(C) Calculate and/or read items 6 through 40 on the first computation sheet and items 41 through 60 on the second computation sheet.

Item Number

6	ρ/ρ - Density ratio
7	N - Propeller speed (revolutions per minute) - engine speed multiplied by the gear ratio
8	ψ - Angle of Inclination thrust axis makes with inflow velocity (degrees)
9	Cosine ψ
10	J - Propeller advance ratio based on stream-wise component on the velocity = 101.4 (Vk)/(N) (Diameter)
11	J' - Effective advance ratio based on velocity component normal to the propeller disc = J cosine ψ

APPENDIX A (Continued)

Item Number

12 $(1/J')$ - For $J' > 1.0$

13 $(1/J')^2$

14 $N^3 \times 10^{-9}$ - To facilitate solution of Cp (i.e., if N = 1,000, $N^3 \times 10^{-9} = 1.0$)

15 $D^5 \times 10^{-5}$ - To facilitate solution of Cp (i.e., if D = 10, $D^5 \times 10^{-5} = 1.0$)

16 Cp - Power coefficient = $(BHP)(\%)/2000\ (N^3 \times 10^{-9})(D^5 \times 10^{-5})$

17 C_Q - Torque coefficient = $Cp/2\pi$

18 Q_c - Torque coefficient for $J' > 1.0$ = $(C_Q)(1/J')^2$

19 $(4/B).83$ - Number of blade correction to torque coefficient, Figure A1.

20 Q_{AF} - Activity factor correction to torque coefficient, Figure A1

21 C''_Q or Q''_C - Effective torque coefficient (corrected for 4 blades and 140 activity factor) = C_Q or Q_C multiplied by Q_{AF} and $(4/B).83$

22 $\Delta C''_Q$ or $\Delta Q''_C$ - Camber correction to torque coefficient (for $J' \leq 1.0$, Figure A2; for $J' > 1.0$, Figure A3)

23 $C'_{Q\,\psi}$ or $Q'_{C\,\psi}$ - Effective torque coefficient (corrected for 4 blades, 140 activity factor and 0.500 integrated design C_L) = $C''_Q - \Delta C''_Q$ or $Q''_C - \Delta Q''_C$

24 K_Q - Inflow correction factor, a function of J', Figure A4.

25 ψ_Q - Inflow correction factor, a function of the inflow angle, Figure A5.

26 $(K_Q)(\psi_Q)$ - Inflow correction factor to torque coefficient

27 C'_Q or Q'_C - Effective torque coefficient (corrected for 4 blades, 140 activity factor, 0.500 integrated design C_L and zero inflow angle) = $C'_{Q\,\psi}$ or $Q'_{C\,\psi}$ minus $(K_Q)(\psi_Q)$

28 θ 3/4 - Blade angle at three-quarter radius (for $J' \leq 1.0$, read from Figure A6; for $J' > 1.0$ read from Figure A7)

29 C'_T or T'_C - Effective thrust coefficient (for 4 blades, 140 activity factor, 0.500 integrated design C_L and zero inflow angle). For $J' \leq 1.0$, read from Figure A8; for $J' > 1.0$, read from Figure A9.

APPENDIX A (Continued)

Item Number

30 K_T - Inflow correction factor, a function of J', Figure A10

31 Ψ_T - Inflow correction factor, a function of the inflow angle, Figure A11

32 $(K_T)(\Psi_T)$ - Inflow correction factor to thrust coefficient

33 $C'_{T\Psi}$ or $T'_{C\Psi}$ - Effective thrust coefficient (for four blades, 140 activity factor, 0.500 integrated design C_L and the given inflow angle).

34 $\Delta C''_T$ or $\Delta T''_C$ - Camber correction to thrust coefficient (for $J' \leq 1.0$, Figure A12; for $J' > 1.0$, Figure A13).

35 C''_T or T''_C - Effective thrust coefficient (for four blades, 140 activity factor, given integrated design C_L and given inflow angle). = $C'_{T\Psi} + \Delta C''_T$ or $T''_{C\Psi} + \Delta T''_C$

36 $(4/B)^{.83}$ - Number of blade correction to thrust coefficient Figure A14.

37 T_{AF} - Activity factor correction to thrust coefficient, Figure A14.

38 T_C - Thrust coefficient for $J' > 1.0$ = T''_C divided by $(4/B)^{.83}$ and T_{AF}

39 $C_T = T_C/(1/J')^2$ - For $J' > 1.0$; for $J' \leq 1.0$, C''_T divided by $(4/B)^{.83}$ and T_{AF}

40 Thrust - $C_T\ (\rho n^2 D^4)$ or $6610\ C_T\ (N^2 \times 10^{-6})(D^4 \times 10^{-4})(R/\rho)$ (pounds)

41 C'_N or N'_C - Effective normal force coefficient (for four blades, 133 side force factor and 0.500 integrated design C_L at a 45° inflow angle). Figure A15.

42 Tangent Ψ

43 $C'_{N\Psi}$ or $N'_{C\Psi}$ - Effective normal force coefficient (for four blades, 133 side force factor, 0.500 integrated design C_L and the given inflow angle = C'_N or N'_C multiplied by the tangent of the inflow angle.)

44 $\Delta C''_N$ or $\Delta N''_C$ - Camber correction to normal force coefficient. For $J' \leq 1.0$, Figure A16; for $J' > 1.0$, Figure A17.

APPENDIX A (Continued)

Item Number

45 C''_N or M''_C - Effective normal force coefficient (for four blades, 133 side force factor, given integrated design C_L and given inflow angle) = $C'_{n\psi} + \Delta C''_n$ or $M_{C\psi} + \Delta M''_C$

46 N_{SFF} - Side force factor correction to normal force coefficient, Figure A18

47 $(4/B)^{.83}$ - Number of blades correction to normal force coefficient, Figure A18

48 N_C - Normal force coefficient for $J' > 1.0$ = M''_C divided by N_{SFF} and $(4/B)^{.83}$

49 $C_N = N_C/(1/J')^2$ - For $J' > 1.0$; for $J' \leqq 1.0$, $C_N = C''_N$ divided by N_{SFF} and $(4/B)^{.83}$

50 F_N - Normal force $C_N \rho n^2 D^4$ or $(6610)\, C_N\, (n^2 \times 10^{-6})(D^4 \times 10^{-4})(\rho_o/\rho)$ (pounds)

51 C'_M or M'_C - Effective moment coefficient (for four blades, 140 activity factor, 0.500 integrated design C_L at a 45° inflow angle) Figure A19.

52 Tangent ψ

53 $C'_{M\psi}$ or $M'_{C\psi}$ - Effective moment coefficient (for four blades, 140 activity factor, 0.500 integrated design C_L and the given inflow angle.) = C'_M or M'_C multiplied by the tangent of the inflow angle.

54 $\Delta C''_M$ or $\Delta M''_C$ - Camber correction to moment coefficient. For $J' \leqq 1.0$, Figure A20; for $J' > 1.0$, Figure A21.

55 C''_M or M''_C - Effective moment coefficient (for four blades, 140 activity factor and given integrated design C_L and given inflow angle) = $C'_{M\psi} + \Delta C''_M$ or $M'_{C\psi} + \Delta M''_C$

56 M_{AF} - Activity factor correction to moment coefficient, Figure A22.

57 $(4/B)^{.83}$ - Number of blade correction to moment coefficient, Figure A22

58 M_C - Moment coefficient for $J' > 1.0$ = M''_C divided by M_{AF} and $(4/B)^{.83}$

59 $C_M = M_C/(1/J)^2$ for $J' > 1.0$; for $J' \leqq 1.0$, $C_M = C''_M$ divided by M_{AF} and $(4/B)^{.83}$

APPENDIX A (Continued)

Item Number

60 Moment - $C_M \rho n^2 D^5$ or $66{,}100\ C_M\ (M^2 \times 10^{-6})(D^5 \times 10^{-5})/(P/\rho)$ (foot-pounds)

A suggested computation form follows the two sample computation sheets.

HAMILTON STANDARD

AIRPLANE MYTHICAL 1 DATE 3/31/58 CALCULATION No

CALCULATED BY J.F. CHECKED BY S.S.

REFERENCE SAMPLE PROBLEMS

ENGINE T-101 GEAR RATIO 0.100

No. of Blades	4	4	3
Blade	A	B	C
Diameter	10	15	20
A.F.	140	100	180
C_{Li}	.500	.300	.600
S.F.F.	133	100	160

THRUST & TORQUE

				Take-off	Climb	Cruise
[1]	Attitude			Take-off	Climb	Cruise
[2]	BHP			4,000	2,500	5,000
[3]	N_E			20,000	10,000	9,000
[4]	V_{KNOTS}			100	150	300
[5]	Altitude			Sea-Level	5,000'	10,000'
[6]	ρ_0/ρ			1.00	1.160	1.354
[7]	N		[3] Gear Ratio	2000	1,000	900
[8]	ψ			30°	60°	0°
[9]	$\cos\psi$			0.866	0.500	1.0
[10]	J		101.4 [4]/[7] Diameter	0.507	1.014	1.69
[11]	J'		[10][9]	0.440	0.507	1.69
[12]	$1/J'$		for $J' > 1.0$	—	—	0.591
[13]	$(1/J')^2$			—	—	0.350
[14]	$N^3 \times 10^{-9}$			8.00	1.00	0.729
[15]	$D^5 \times 10^{-5}$			1.00	7.594	32.0
[16]	C_P		[2][6]/2000 [14][15]	0.2500	0.1910	0.1455
[17]	C_Q		[16]/2π	0.0398	0.0304	0.0231
[18]	Q_C		[17][13]	—	—	0.00908
[19]	$(4/B)^{.83}$	Fig A2		1.0	1.0	1.28
[20]	Q_{AF}	Fig A2		1.0	1.275	0.834
[21]	C_Q° or Q_C°		[17] or [18] × [19][20]	0.0398	0.0388	0.00864
[22]	ΔC_Q° or ΔQ_C°	Fig A2 or A3		0	-0.0043	0.00220
[23]	$C_{Q\psi}$ or $Q_{C\psi}$		[21]-[22]	0.0398	0.0431	0.00644
[24]	K_Q	Fig A4		.00124	0.00150	0.01250
[25]	ψ_Q	Fig A5		.33	3.02	0
[26]	$[K_Q][\psi_Q]$		[24][25]	0.0004	0.0045	0
[27]	C_Q or Q_C		[23]-[26]	0.0394	0.0386	0.00644
[28]	$\theta_{3/4}$	Fig A6 or A7		25.4°	25.5°	33.6°
[29]	C_T° or T_C°	Fig A8 or A9		0.274	0.262	0.019
[30]	K_T	Fig A10		0.0063	0.0085	0.0589
[31]	ψ_T	Fig A11		0.365	2.77	0
[32]	$[K_T][\psi_T]$		[30][31]	0.0023	0.0236	0
[33]	$C_{T\psi}$ or $T_{C\psi}$		[29]+[32]	0.2763	0.2856	0.019
[34]	ΔC_T° or ΔT_C°	Fig A12 or A13		0	-0.0296	+0.006
[35]	C_T° or T_C°		[33]+[34]	0.2763	0.2560	0.025
[36]	$(4/B)^{.83}$	Fig A14		1.0	1.0	1.28
[37]	T_{AF}	Fig A14		1.0	1.27	0.857
[38]	T_C		[35]/[36][37] for $J' > 1.0$	—	—	0.0228
[39]	$C_T = C_T/J'^2$		or [35]/[36][37] for $J' \leq 1.0$	0.2763	0.2015	0.0652
[40]	Thrust		6610 $(N^3 \times 10^{-9})(D^4 \times 10^{-4}) C_T / \rho_0/\rho$	7300	5810	4130

H. S. F-62

HAMILTON STANDARD

AIRPLANE MYTHICAL1 DATE 3/31/53 CALCULATION NO.

NO. OF BLADES	4	4	3
BLADE	A	B	C
DIAMETER	10	15	20
A.F.	140	100	180
C_{L_i}	.500	.300	.600
S.F.F.	133	100	160

CALCULATED BY JF CHECKED BY S.S.

REFERENCE SAMPLE PROBLEMS

ENGINE T-101 GEAR RATIO 0.100

NORMAL FORCE & SHAFT MOMENT

	J' OR 'IJ'			0.440	0.507	0.591
	Q 3/4			25.4°	25.5°	33.6°
[41]	C'_N OR N'_C	FIG A15		0.0304	0.0356	—
[42]	TAN ψ			0.577	1.732	—
[43]	$C'_{N\psi}$ OR $N'_{C\psi}$		[41][42]	0.01751	0.0617	—
[44]	$\Delta C'_N$ OR $\Delta N'_C$	FIG A16, A17		0	-0.00265	—
[45]	C''_N OR N''_C		[43]+[44]	0.01751	0.05905	—
[46]	NSEFF	FIG A18		1.0	1.262	—
[47]	$(4/B)^{83}$	FIG A18		1.0	1.0	—
[48]	N_C		[45]/[46][47]	—	—	—
[49]	$C_N = N_C/(J')^2$		FOR $J' > 1.0$ OR $\frac{[45]}{[46][47]}$	0.01751	0.0468	—
[50]	FN		(REFER TO FORMULA BELOW)	463	1350	0
[51]	C'_M OR M'_C	FIG A19		0.0215	0.0251	—
[52]	TAN ψ			0.577	1.732	—
[53]	$C'_{M\psi}$ OR $M'_{C\psi}$		[51][52]	0.01241	0.0434	—
[54]	$\Delta C'_M$ OR $\Delta M'_C$	FIG A20 OR A21		0	-0.0071	—
[55]	C''_M OR M''_C		[53]+[54]	0.01241	0.0363	—
[56]	MAF	FIG A22		1.0	1.31	—
[57]	$(4/B)^{83}$	FIG A22		1.0	1.0	—
[58]	M_C		[55]/[56][57]	—	—	—
[59]	$C_M = M_C/(J')^3$		FOR $J' > 1.0$ OR $\frac{[55]}{[56][57]}$	0.01241	0.0277	—
[60]	MOMENT		(REFER TO FORMULA BELOW)	3,285	11,990	0

$$J = \frac{101.4\ V_{KNOTS}}{ND} \qquad C_P = \frac{BHP(60/\rho)}{2000(N^3\times10^{-9})(D^5\times10^5)}$$

$$J' = J\cos\psi$$

$$\text{THRUST} = \frac{6610(N^2\times10^{-6})(D^4\times10^{-4})C_T}{\rho_0/\rho}\ (\text{LBS.})$$

$$F_N = \frac{6610(N^2\times10^{-6})(D^4\times10^{-4})C_N}{\rho_0/\rho}\ (\text{LBS})$$

$$\text{MOMENT} = C_M\rho n^2 D^5 \quad \text{OR} \quad \frac{66{,}100(N^2\times10^{-6})(D^5\times10^{-5})C_M}{\rho_0/\rho}\ (\text{FT. LBS})$$

HAMILTON STANDARD

AIRPLANE DATE CALCULATION NO.

No. OF BLADES			
BLADE			
DIAMETER			
A.F.			
C_{L_i}			
S.F.			

CALCULATED BY CHECKED BY

REFERENCE

ENGINE GEAR RATIO

THRUST & TORQUE

[1]	ATTITUDE			
[2]	B.H.P.			
[3]	N.E.			
[4]	V KNOTS			
[5]	ALTITUDE			
[6]	ρ_o/ρ			
[7]	N			
[8]	ψ			
[9]	$\cos\psi$			
[10]	J			
[11]	J'			
[12]	'1/J'			
[13]	$(1/J')^2$			
[14]	$N^3 \times 10^{-9}$			
[15]	$D^5 \times 10^{-5}$			
[16]	C_P			
[17]	C_Q			
[18]	Q_C			
[19]	$(4/B)^{.83}$			
[20]	Q_{AF}			
[21]	C''_{Q} OR Q''_C			
[22]	$\Delta C''_Q$ OR $\Delta Q''_C$			
[23]	$C_{Q\psi}$ OR $Q'_{C\cdot\psi}$			
[24]	K_Q			
[25]	ψ_Q			
[26]	$[K_Q][\psi_Q]$			
[27]	C_Q OR Q'_C			
[28]	Q 3/4			
[29]	C_T OR T_C			
[30]	K_T			
[31]	ψ_T			
[32]	$[K_T][\psi_T]$			
[33]	$C'_{T\psi}$ OR $T'_{C\cdot\psi}$			
[34]	$\Delta C''_T$ OR $\Delta T''_C$			
[35]	C''_T OR T''_C			
[36]	$(4/B)^{.83}$			
[37]	TAE			
[38]	TC			
[39]	$C_T = T_C/(N/1000)^2$			
[40]	THRUST			

NORMAL FORCE & SHAFT MOMENT

	J' OR 'kJ'			
	Q 3/4			
[41]	C'_N OR N'_C			
[42]	TAN ψ			
[43]	$C'_{N\psi}$ OR $N'_{C\cdot\psi}$			
[44]	$\Delta C''_N$ OR $\Delta N''_C$			
[45]	C''_N OR N''_C			
[46]	N SEE			
[47]	$(4/B)^{.83}$			
[48]	NC			
[49]	$C_N = N_C/(N/1000)^2$			
[50]	FN			
[51]	C'_M OR M'_C			
[52]	TAN ψ			
[53]	$C'_{M\psi}$ OR $M'_{C\cdot\psi}$			
[54]	$\Delta C''_M$ OR $\Delta M''_C$			
[55]	C''_M OR M''_C			
[56]	MAF			
[57]	$(4/B)^{.83}$			
[58]	MC			
[59]	$C_M = M_C/(N/1000)^2$			
[60]	MOMENT			

$J = \frac{101.4\ V_{KNOTS}}{N'D}$ $\quad C_P = \frac{BHP \times \rho_o/\rho}{2000 \times (N \times 2.10^{-4})^3 (D \times 10^{-5})^5}$

$J' = J\cos\psi$

$THRUST = \frac{66.10 (N^2 \times 10^{-4})(D^4 \times 10^{-4})}{\rho_o/\rho} C_T$ (LBS.)

$FN = \frac{66.10 (N^2 \times 10^{-4})(D^4 \times 10^{-4})}{\rho_o/\rho} C_N$ (LBS.)

$MOMENT = \frac{66.10 (N^2 \times 10^{-4})(D^5 \times 10^{-5})}{\rho_o/\rho} C_M$ (FT. LBS.)

M. S. F-62

HAMILTON STANDARD

WINDSOR LOCKS, CONNECTICUT, U.S.A.

HS-1829

FIGURE A1

EFFECT OF ACTIVITY FACTOR ON TORQUE COEFFICIENT

$$C_{QB} = C_Q \times (4/B)^{.85} \times Q_{AF}$$

$$Q_{CB} = Q_C \times (4/B)^{.85} \times Q_{AF}$$

NO. OF BLADE CORRECTION

B	$(4/B)^{.85}$
3	1.28
4	1.00

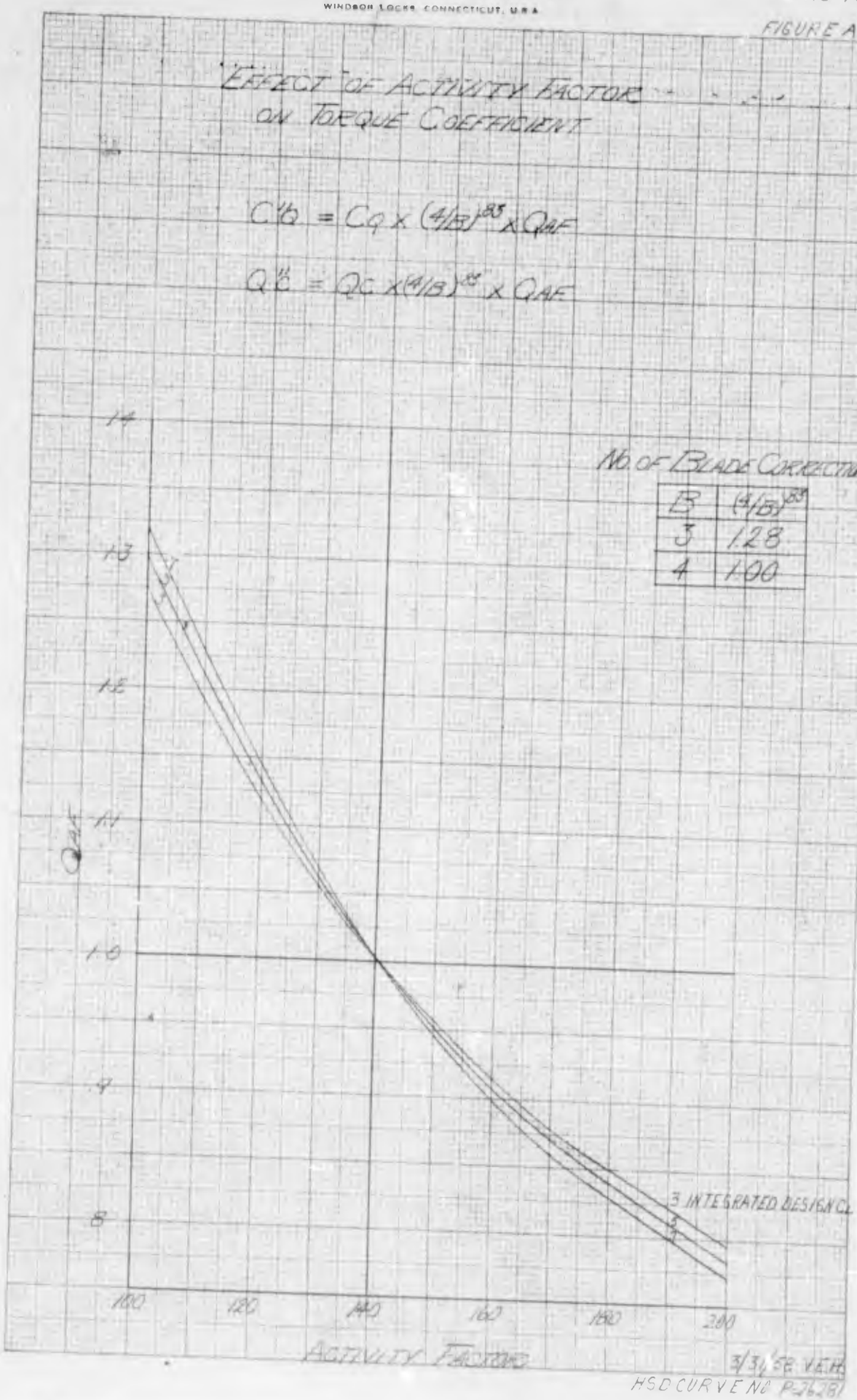

3/3 SE VEH

HSD CURVE NO P-76281

PAGE 54

KEUFFEL & ESSER CO. 359-11 10 X 10 TO THE ½ INCH

HAMILTON STANDARD DIVISION

WINDSOR LOCKS, CONNECTICUT, U. S. A.

HS-1829

FIGURE A-2

EFFECT OF INTEGRATED DESIGN CL ON TORQUE COEFFICIENT FOR $J' \leq 1.0$

$$C_{Q}^{J'=1.0} = C_{Q} - \Delta C_{Q}$$

$$\Delta C_{Q} = \left(\Delta C_{Q} \text{ CHART}\right)\left(\frac{C_L - .500}{.200}\right)$$

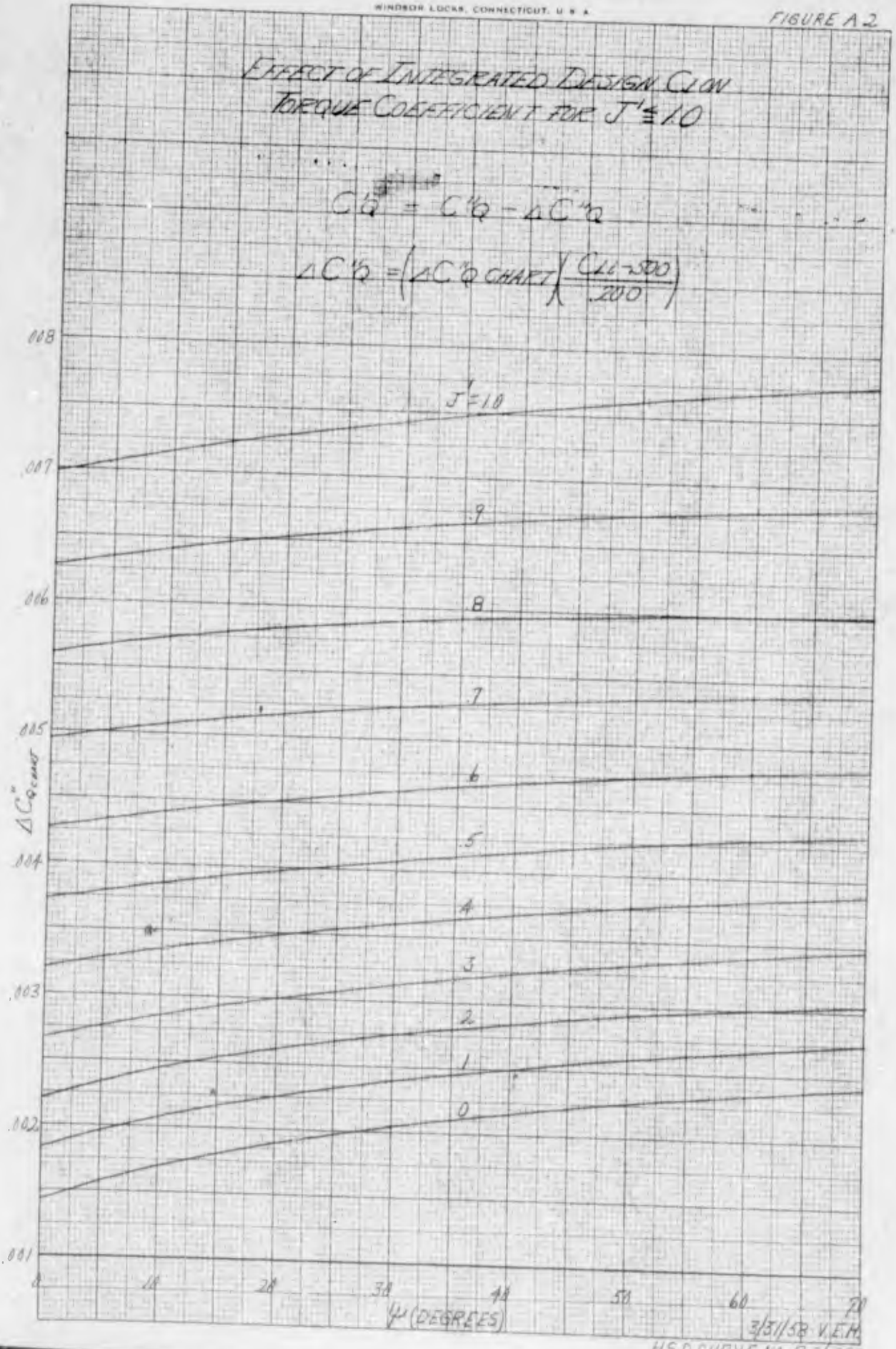

3/31/58 V.E.H.

HSD CURVE NO P-26282

HAMILTON STANDARD DIVISION

WINDSOR LOCKS, CONNECTICUT, U. S. A.

HS-1829

FIGURE A 3

EFFECT OF INTEGRATED DESIGN C_L ON TORQUE COEFFICIENT FOR $J' \geq 1.0$

$$Q'_C = Q'_C - \Delta Q'_C$$

$$\Delta Q'_C = \left(\Delta Q''_C \text{ CHART}\right)\left(\frac{C_{L_i} - .500}{.200}\right)$$

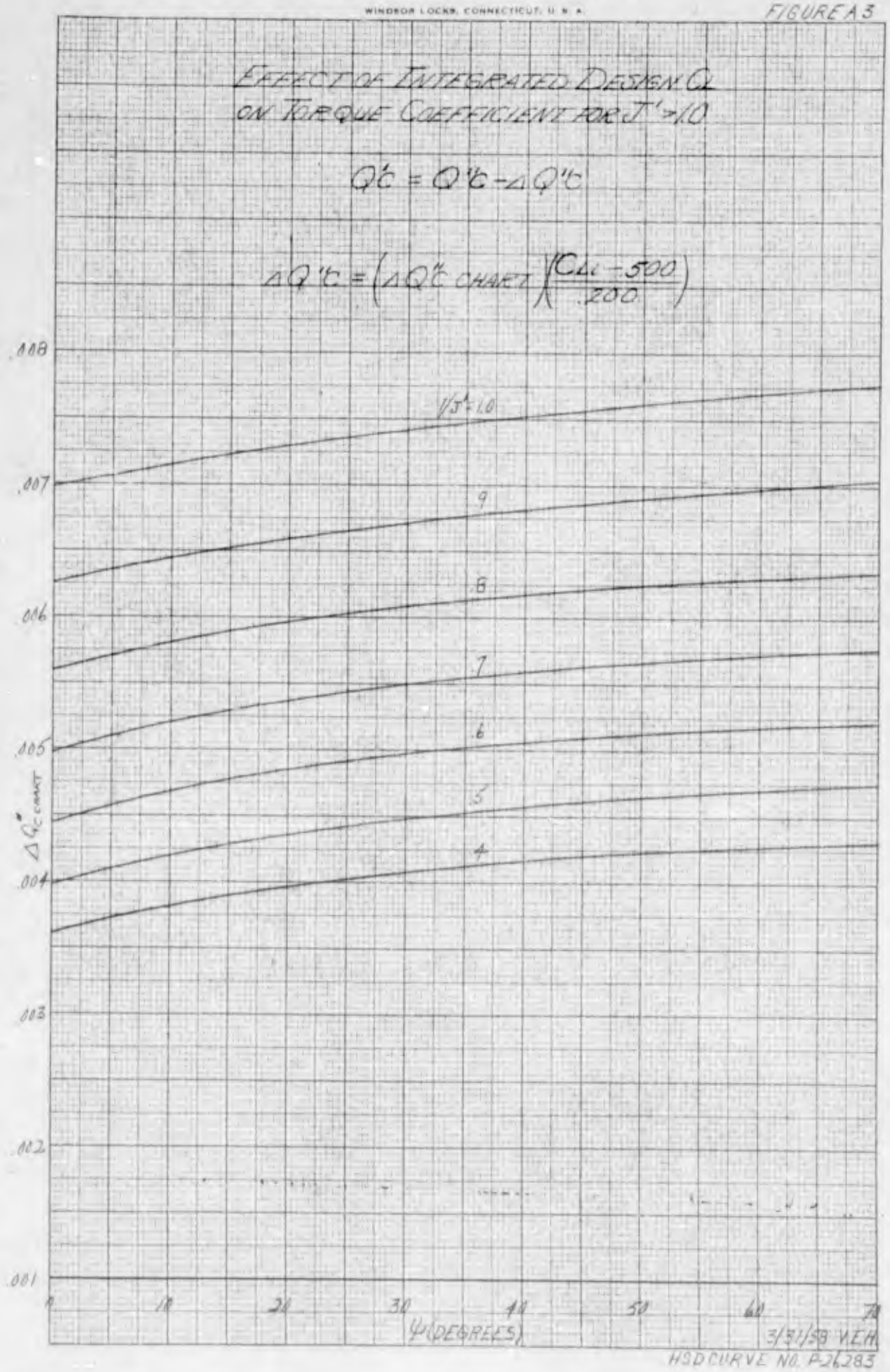

3/31/58 V.E.H.

HSD CURVE NO. P-26283

10 X 10 TO THE ½ INCH 359-11
KEUFFEL & ESSER CO

HS. F 190A 4-53

HAMILTON STANDARD DIVISION

WINDSOR LOCKS, CONNECTICUT, U. S. A.

FIGURE A4

VARIATION OF K_Q WITH J (& $1/J$)

$$Qt_4 = Qt + (K_Q)(\Psi_Q)$$

$$C'_{Q_4} = C'_Q + (K_Q)(\Psi_Q)$$

FOR VALUES OF Ψ_Q REFER TO FIGURE A5

$1/J$

J

K_Q

0 .002 .004 .006 .008 .010 .012 .014

3/21/58 V.E.H.
HSD CURVE NO. P-26284

HAMILTON STANDARD

WINDSOR LOCKS CONNECTICUT, U.S.A.

HS-18.29

FIGURE A5

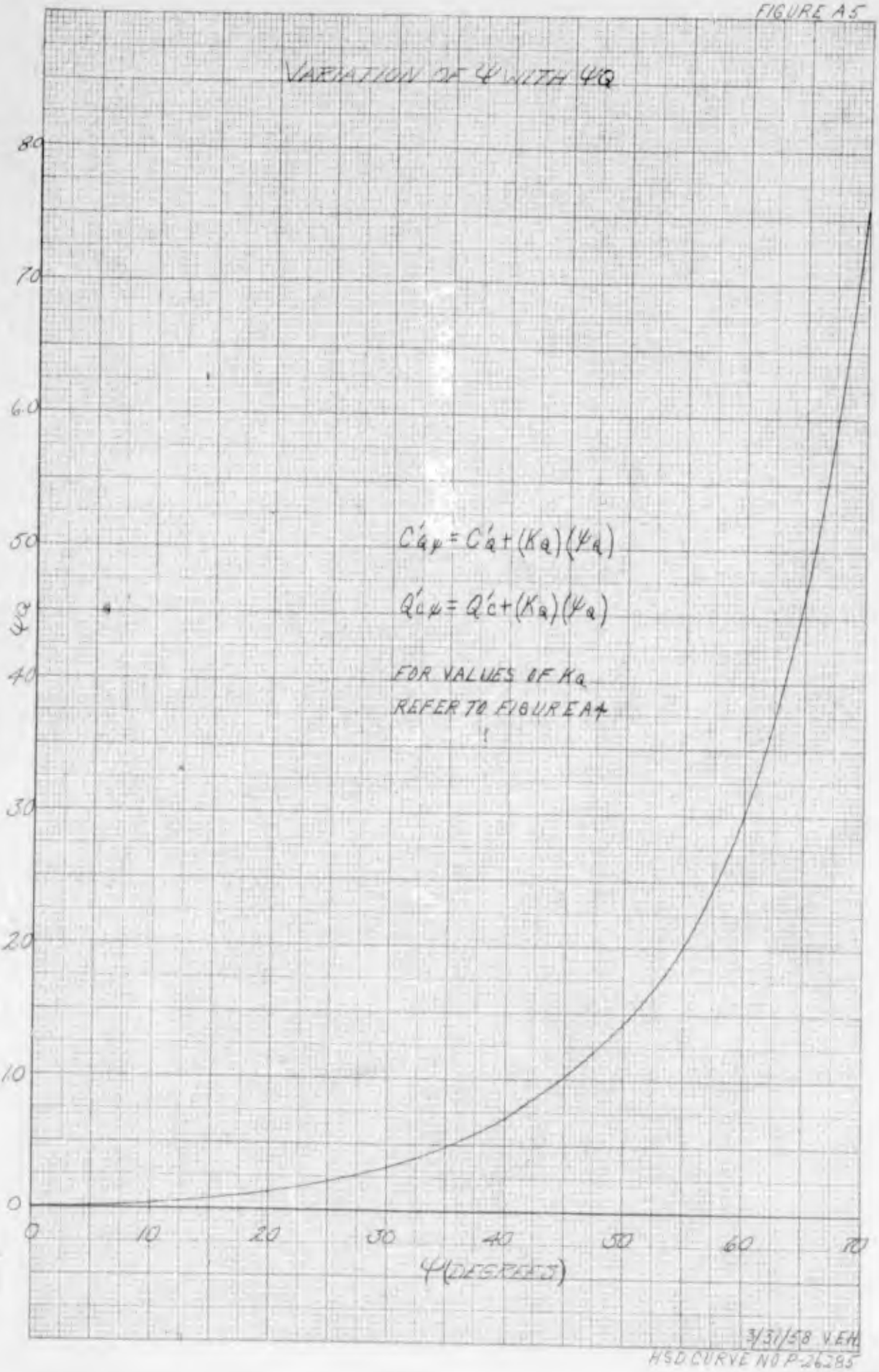

3/31/58 V.E.H.

HSD CURVE NO P-26285

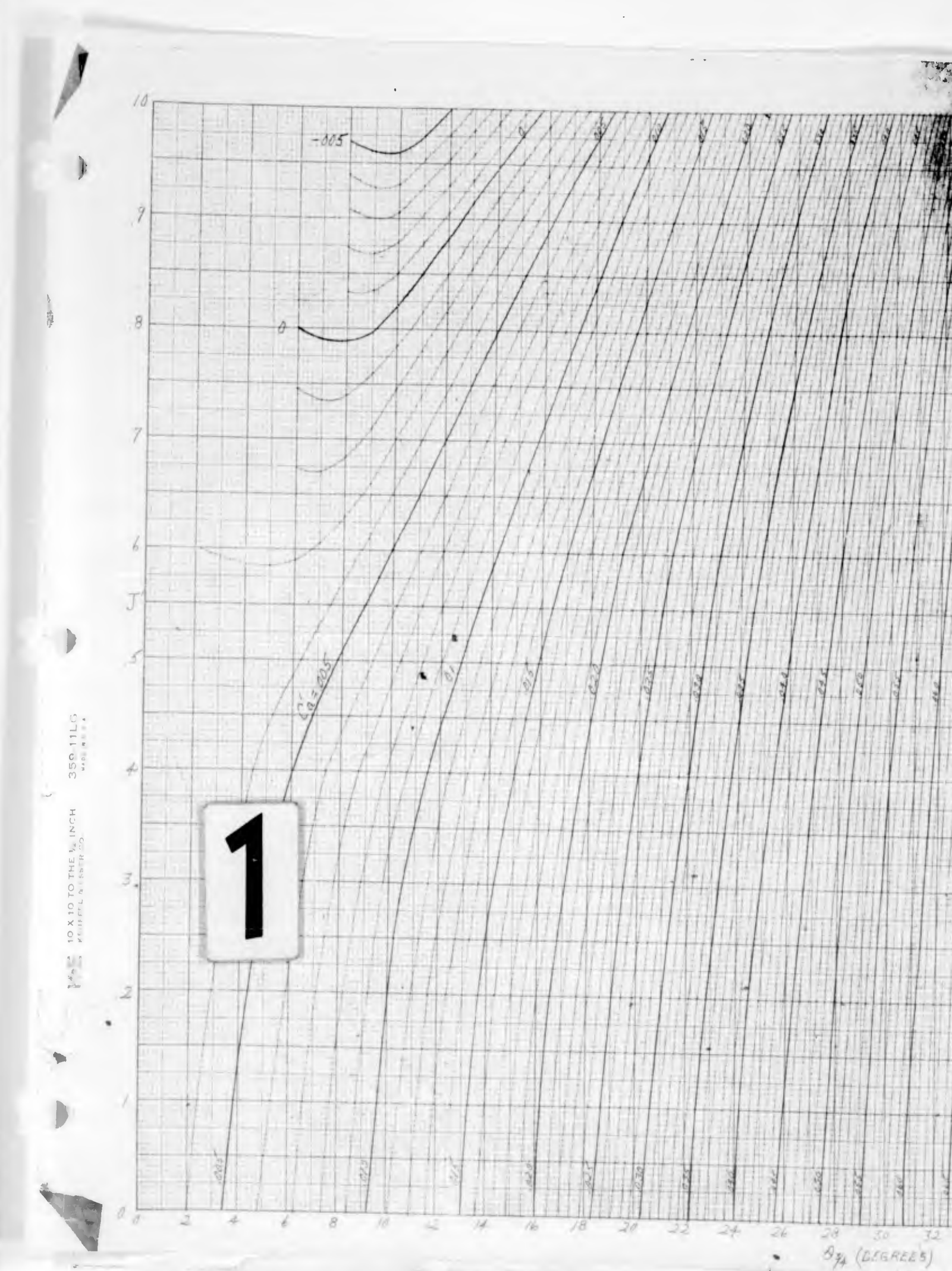
-.005
0
$C_T = .005$
J
$\theta_{3/4}$ (DEGREES)
10 X 10 TO THE ½ INCH
KEUFFEL & ESSER CO
359-11LG

FIGURE A6

C'_Q VS. J' & $\theta_{3/4}$

VARIATION OF EFFECTIVE ADVANCE RATIO WITH EFFECTIVE TORQUE COEFFICIENT AT ZERO INFLOW ANGLE AND WITH BLADE ANGLE FOR $J' \leq 1.0$

FOR A 4-BLADED SINGLE ROTATION PROPELLER, INCORPORATING NACA 16-SERIES AIRFOIL SECTIONS, ACTIVITY FACTOR OF 140 AND AN INTEGRATED DESIGN C_i OF 0.500

C'_Q = EFFECTIVE C_Q @ $\psi = 0°$
$= C''_Q - \Delta C''_Q$

$C''_Q = C_Q \times (1/B)^{.83} \times Q_{AF}$

$C'_{Q\psi}$ = EFFECTIVE C_Q @ ψ
$= C'_Q + (K_Q)(\psi_Q)$

J' = EFFECTIVE J

$J = V/nD$

$J' = J \cos\psi$

2

30 32 34 36 38 40 42 44 46 48 50 52 54 56 58 60

$\theta_{3/4}$ (DEGREES)

3/31/58 VEH PAS/31
HSD CURVE NO P-26286

VARIATION OF EFFECTIVE ADVANCE RATIO WITH EFFECTIVE TORQUE COEFFICIENT AT ZERO INFLOW ANGLE AND WITH BLADE ANGLE FOR $J' > 1.0$

FOR A 4-BLADED SINGLE ROTATION PROPELLER, INCORPORATING NACA 16-SERIES AIRFOIL SECTIONS, ACTIVITY FACTOR OF 140 AND AN INTEGRATED DESIGN C_L OF 0.500

Q'_c = EFFECTIVE Q_c @ $\psi = 0°$
$= (C'_q)(J')^2$
$= Q''_c - \Delta Q''_c$

$Q''_c = Q_c \times (J')^{.85} \times Q_{AF}$

$Q'_{c\psi}$ = EFFECTIVE Q_c @ ψ
$= Q'_c + (K_a)(\psi_a)$

J' = EFFECTIVE J

$J = V/nD$

$J' = J \cos\psi$

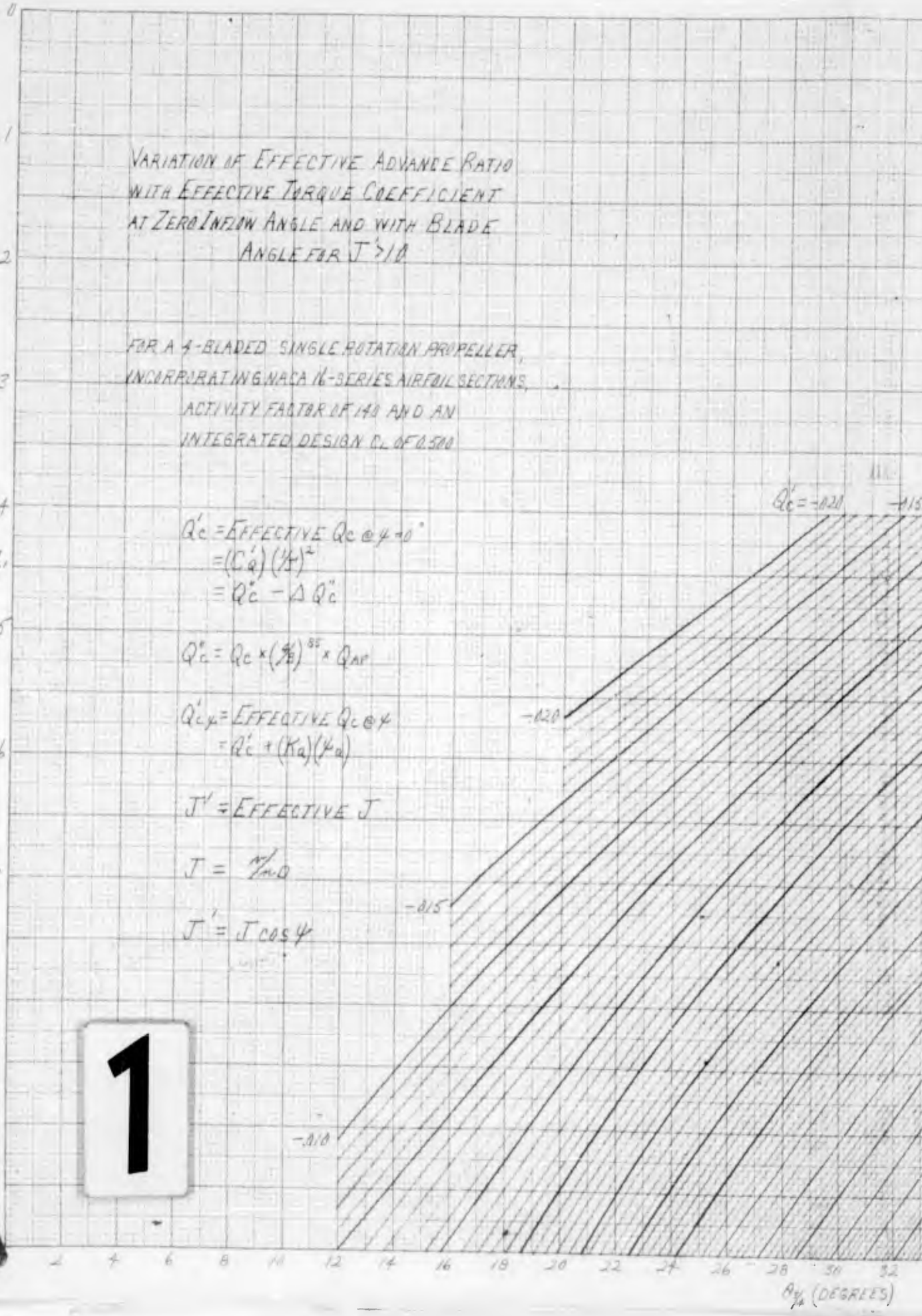

1

HS-1829

FIGURE A7

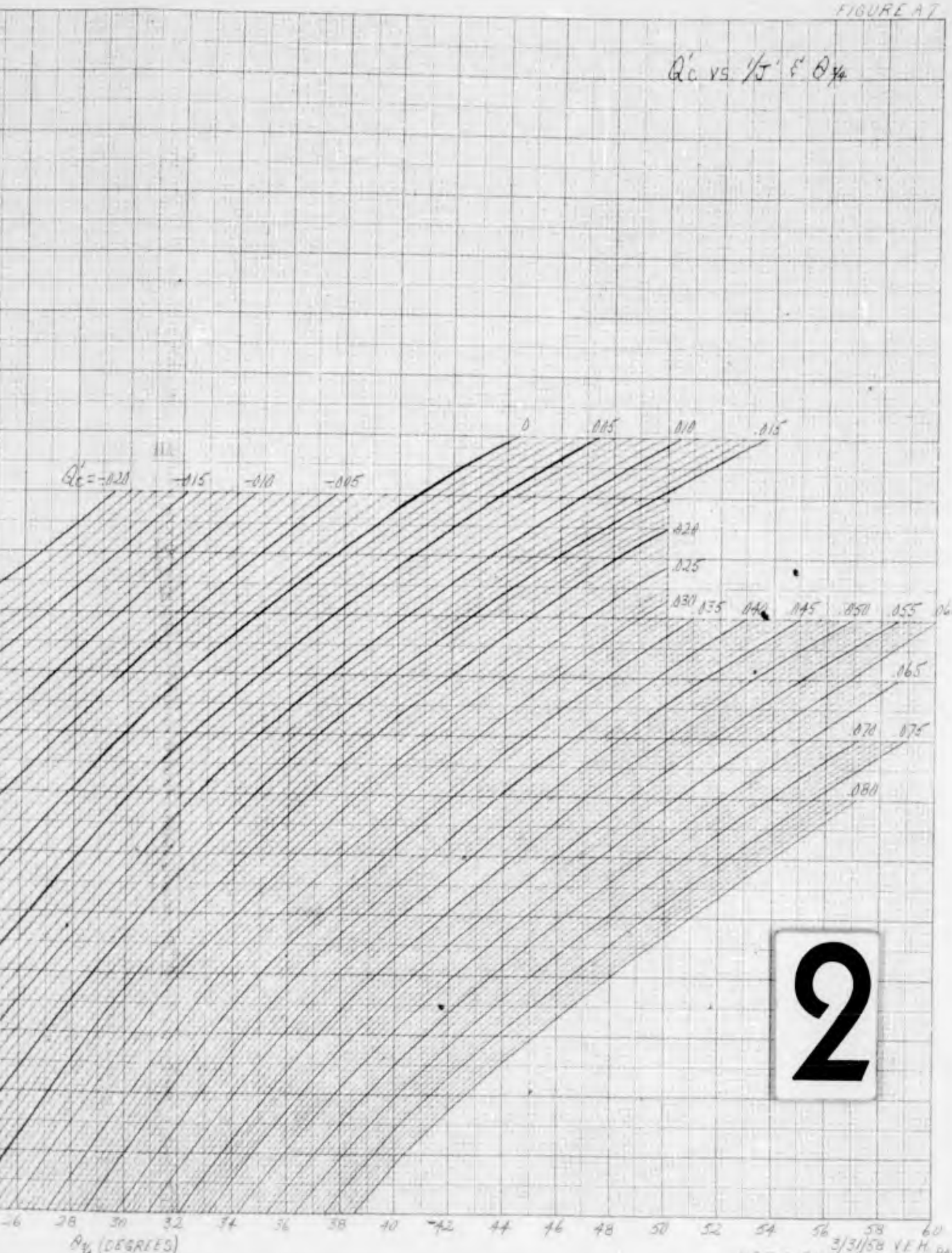

2

3/31/58 V.E.H.
HSD CURVE NO P-26287 PAGE 32

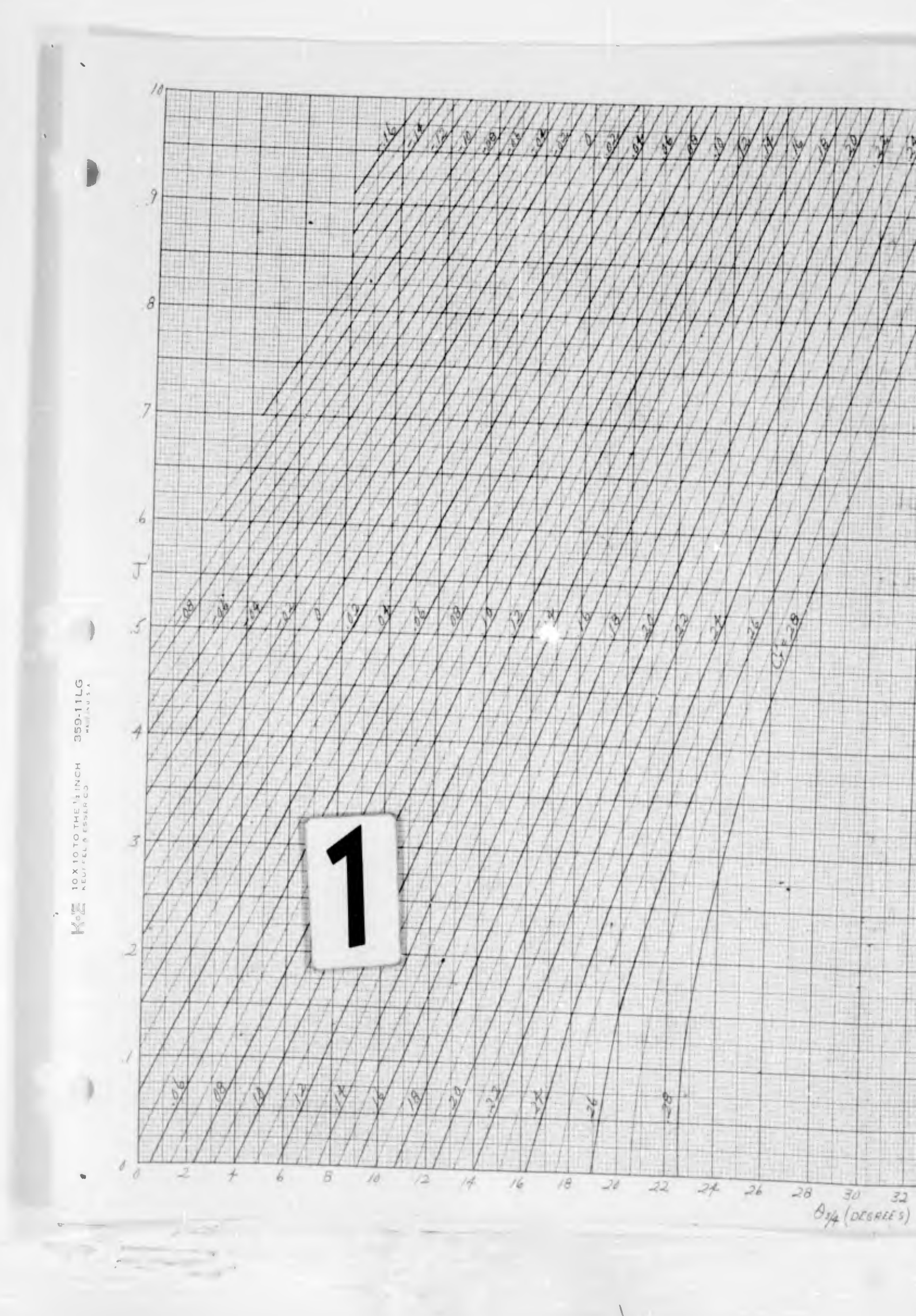
10 X 10 TO THE ½ INCH
KEUFFEL & ESSER CO
359-11LG
MADE IN U.S.A.
1
$\alpha_{3/4}$ (DEGREES)
$C_L = .28$

FIGURE A8

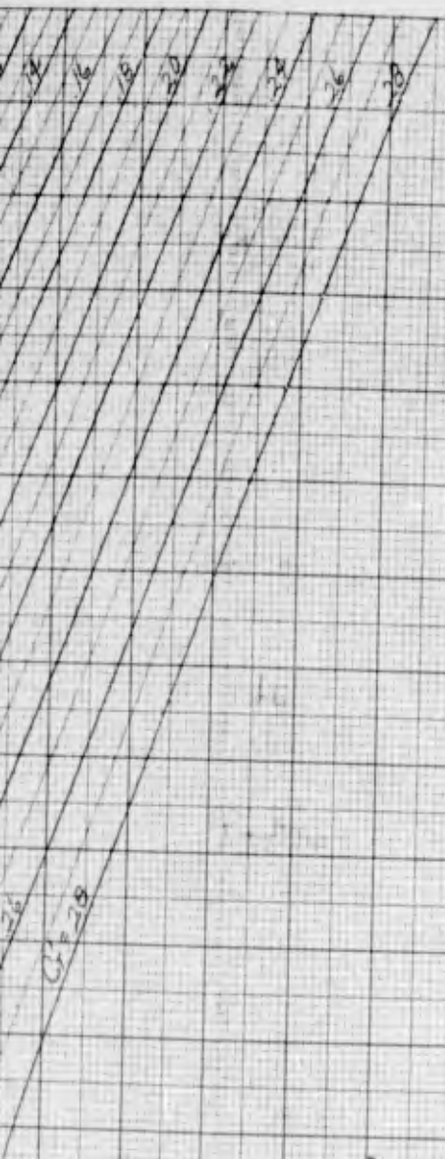

VARIATION OF EFFECTIVE ADVANCE RATIO WITH EFFECTIVE THRUST COEFFICIENT AT ZERO INFLOW ANGLE AND WITH BLADE ANGLE FOR $J' \leq 1.0$

FOR A 4-BLADED SINGLE ROTATION PROPELLER, INCORPORATING 6 NACA 16-SERIES AIRFOIL SECTIONS, ACTIVITY FACTOR OF 140 AND AN INTEGRATED DESIGN C_L OF 0.500

C_T' = EFFECTIVE C_T @ $\psi=0°$
$= C_T'' + \Delta C_T''$

$C_T'' = C_T \times \left(\frac{\sigma}{\sigma_{.75}}\right)^{.83} \times T_{AF}$

C_{T_ψ}'' = EFFECTIVE C_T @ ψ
$= C_T' + (K_T)(V_T)$

J' = EFFECTIVE J

$J = \frac{V}{nD}$

$J' = J \cos\psi$

2

VARIATION OF EFFECTIVE ADVANCE RATIO WITH EFFECTIVE THRUST COEFFICIENT AT ZERO INFLOW ANGLE AND WITH BLADE ANGLE FOR $J' \geq 1.0$

FOR A 4-BLADED SINGLE ROTATION PROPELLER, INCORPORATING NACA 16-SERIES AIRFOIL SECTIONS, ACTIVITY FACTOR OF 140 AND AN INTEGRATED DESIGN C_L OF 0.500

T_c' = EFFECTIVE T_c @ $\psi = 0°$
$= (C_T')(K_T)^2$
$= T_c'' - \Delta T_c''$

$T_c'' = T_c \times (\frac{1}{B})^{.83} \times T_{AA}$

$T'_{c\psi}$ = EFFECTIVE T_c @ ψ
$= T_c' + (K_{T_1})(\psi_1)$

J' = EFFECTIVE J

$J = V/nD$

$J' = J \cos \psi$

$T_c' =$ -.16 -.14 -.12

$\beta_{3/4}$ (DEGREES)

1

FIGURE A9

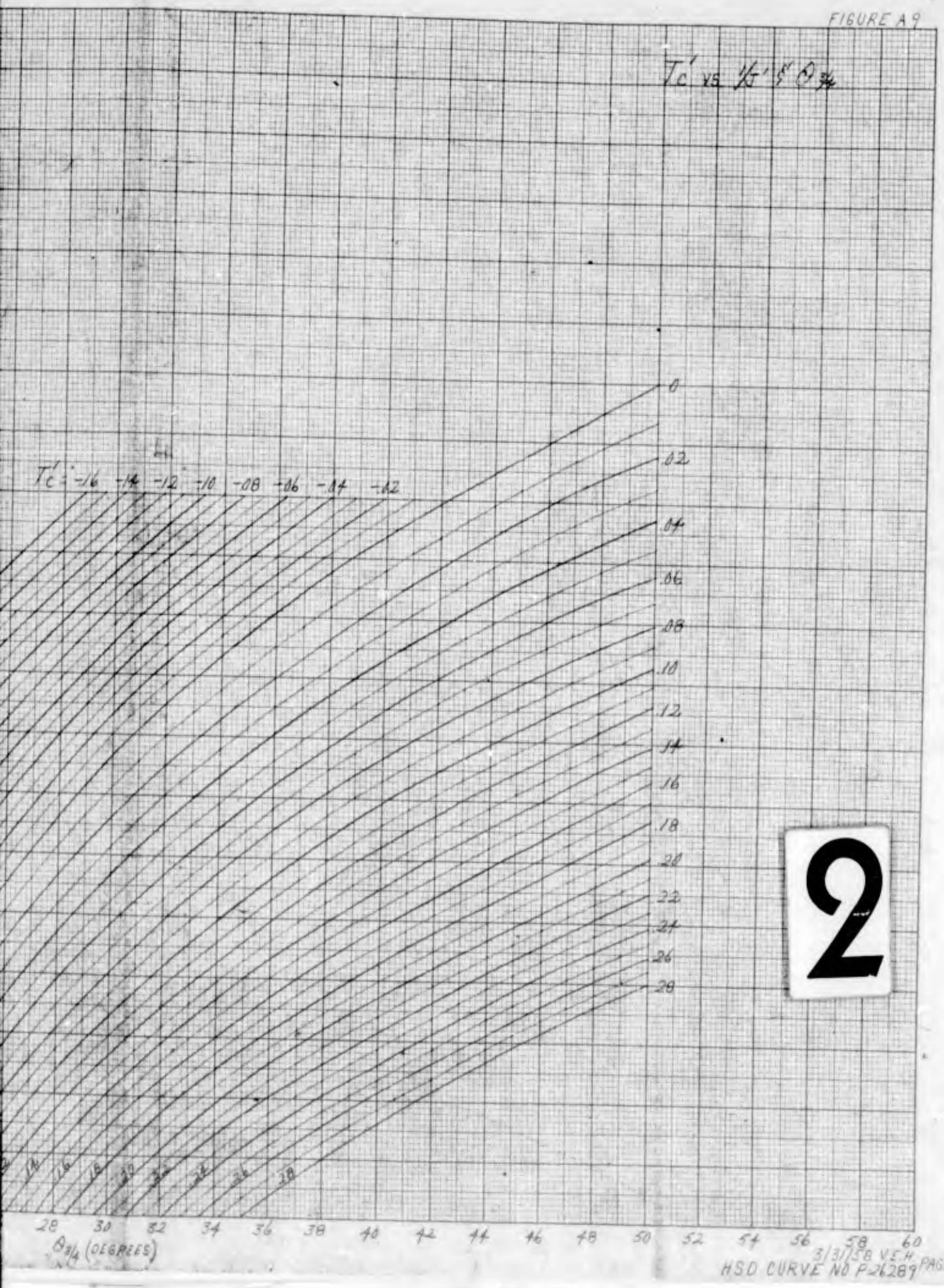

2

3/31/58 V.E.H.
HSD CURVE NO P-26289

FIGURE A 10

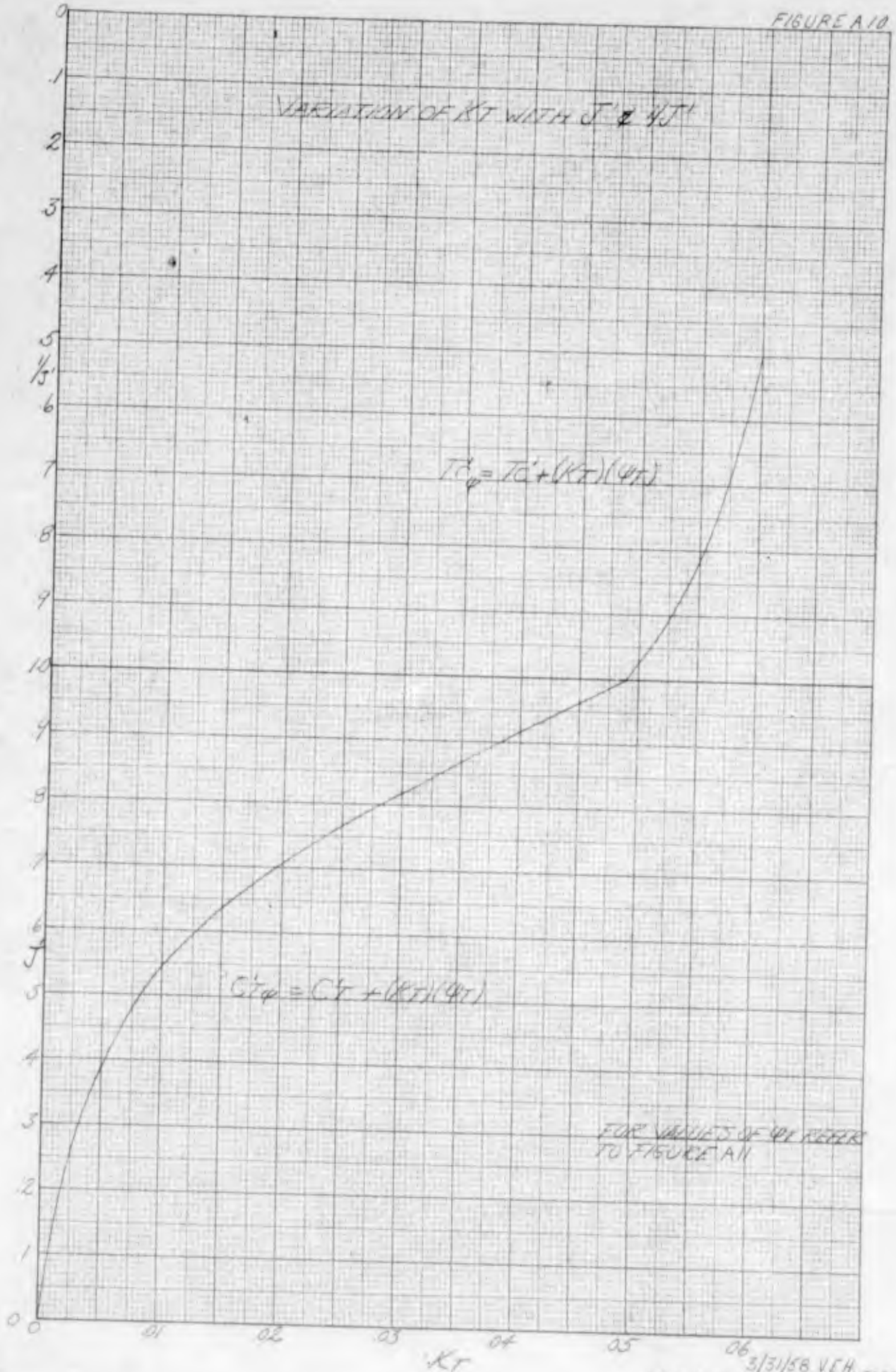

3/31/58 V.E.H.

HSD CURVE NO. P-26290

HAMILTON STANDARD

WINDSOR LOCKS, CONNECTICUT, U.S.A.

HS-1829

FIGURE A11

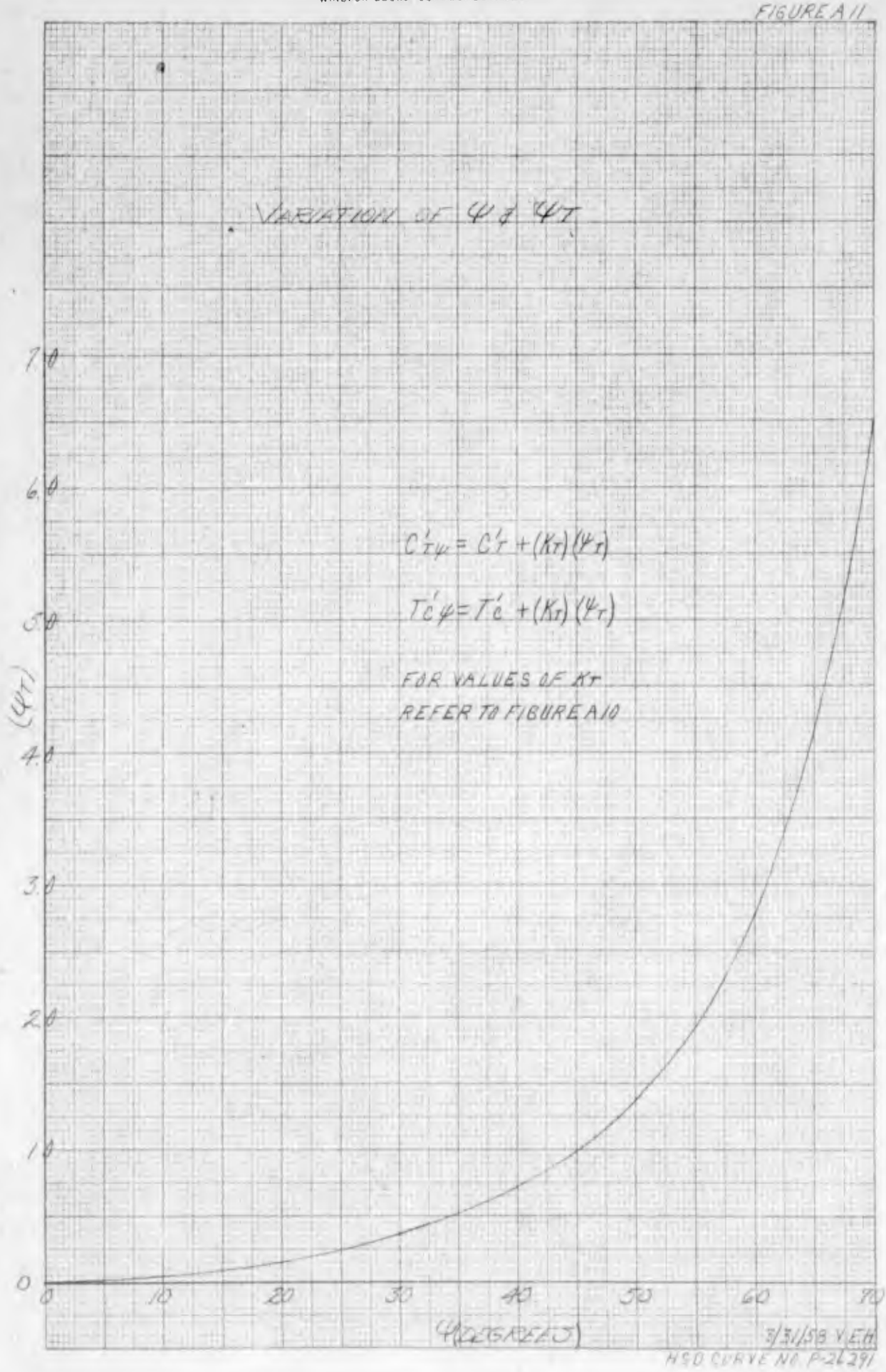

3/31/58 V.E.H.

HSD CURVE NO. P-26291

PAL

HS. F-1808 4-57

FIGURE A12

HAMILTON STANDARD DIVISION

WINDSOR LOCKS, CONNECTICUT, U. S. A.

EFFECT OF INTEGRATED DESIGN C_L ON THRUST COEFFICIENT FOR $J' \leq 1.0$

$$C_T' = C_T'' - \Delta C_T''$$

$$\Delta C_T'' = \left(\Delta C_T''_{CHART}\right)\left(\frac{C_{L_i} - .500}{.200}\right)$$

$J'=1.0$

.9
.8
.7
.6
.5
.4
.3
.2
.1
.0

$\Delta C_{T_{CHART}}''$

.036
.032
.028
.024
.020
.016
.012
.008
.004

0 10 20 30 40 50 60 70

Ψ (DEGREES)

3/31/58 YEH

HSD CURVE NO P2L2-2

HS. F.1804 4-53

HAMILTON STANDARD DIVISION

WINDSOR LOCKS, CONNECTICUT, U. S. A.

FIGURE A-3

EFFECT OF INTEGRATED DESIGN C_L ON THRUST COEFFICIENT FOR $J' > 1.0$

$$T_C' = T_C - \Delta T_C''$$

$$\Delta T_C'' = (\Delta T_C'' \text{ CHART})\left(\frac{C_{L_i} - .500}{.200}\right)$$

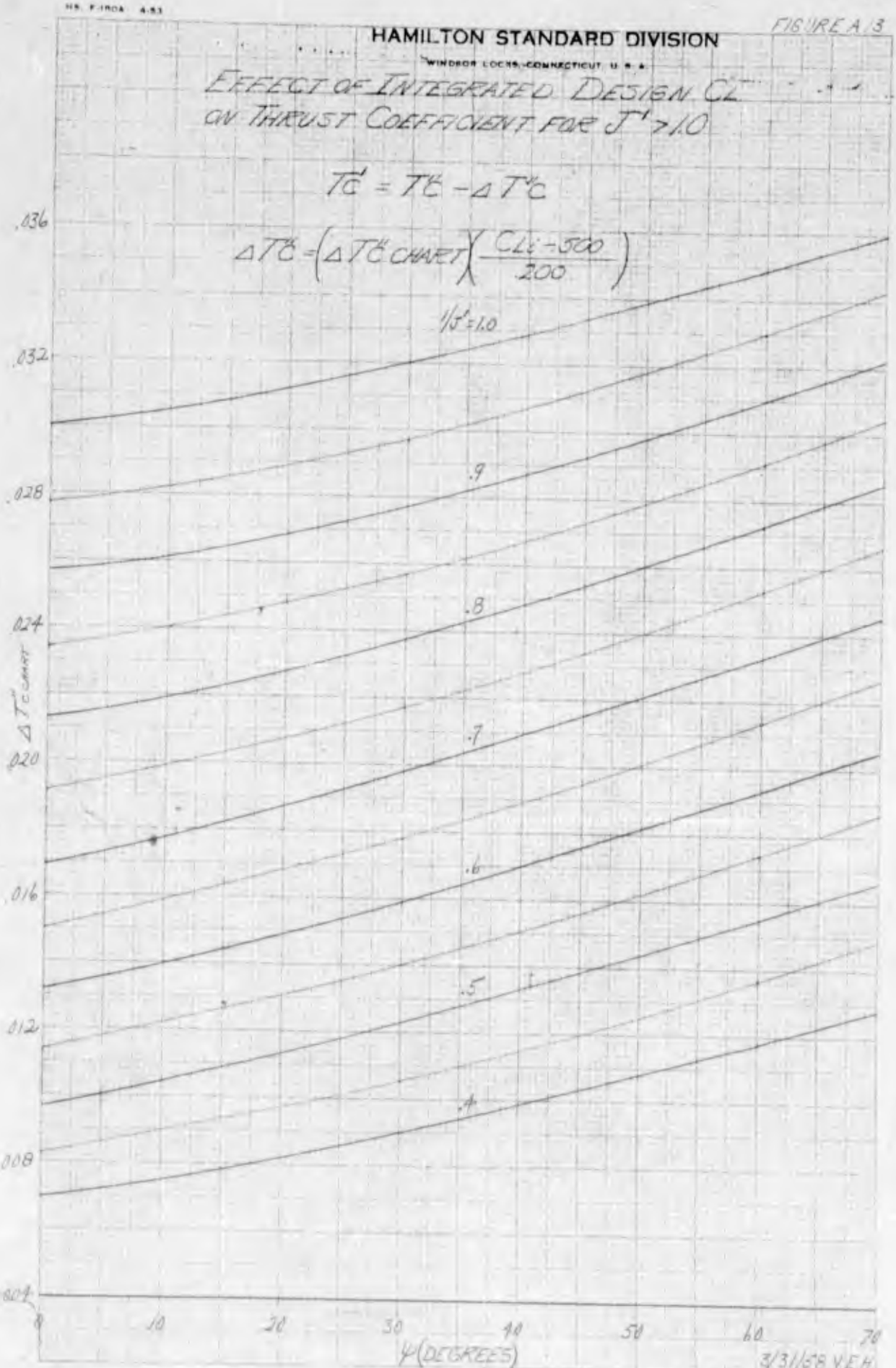

3/31/58 V.E.H.

HSD CURVE NO. P-26393

EFFECT OF ACTIVITY FACTOR ON THRUST COEFFICIENT

$$C_T' = C_T \times (\sigma/\sigma_1)^{.33} \times T_{AF}$$

$$T_C = T_C \times (\sigma/\sigma_1)^{.3} \times T_{AF}$$

NO OF BLADE CORRECTION

B	$(\sigma/\sigma_1)^{.33}$
3	1.28
4	1.00

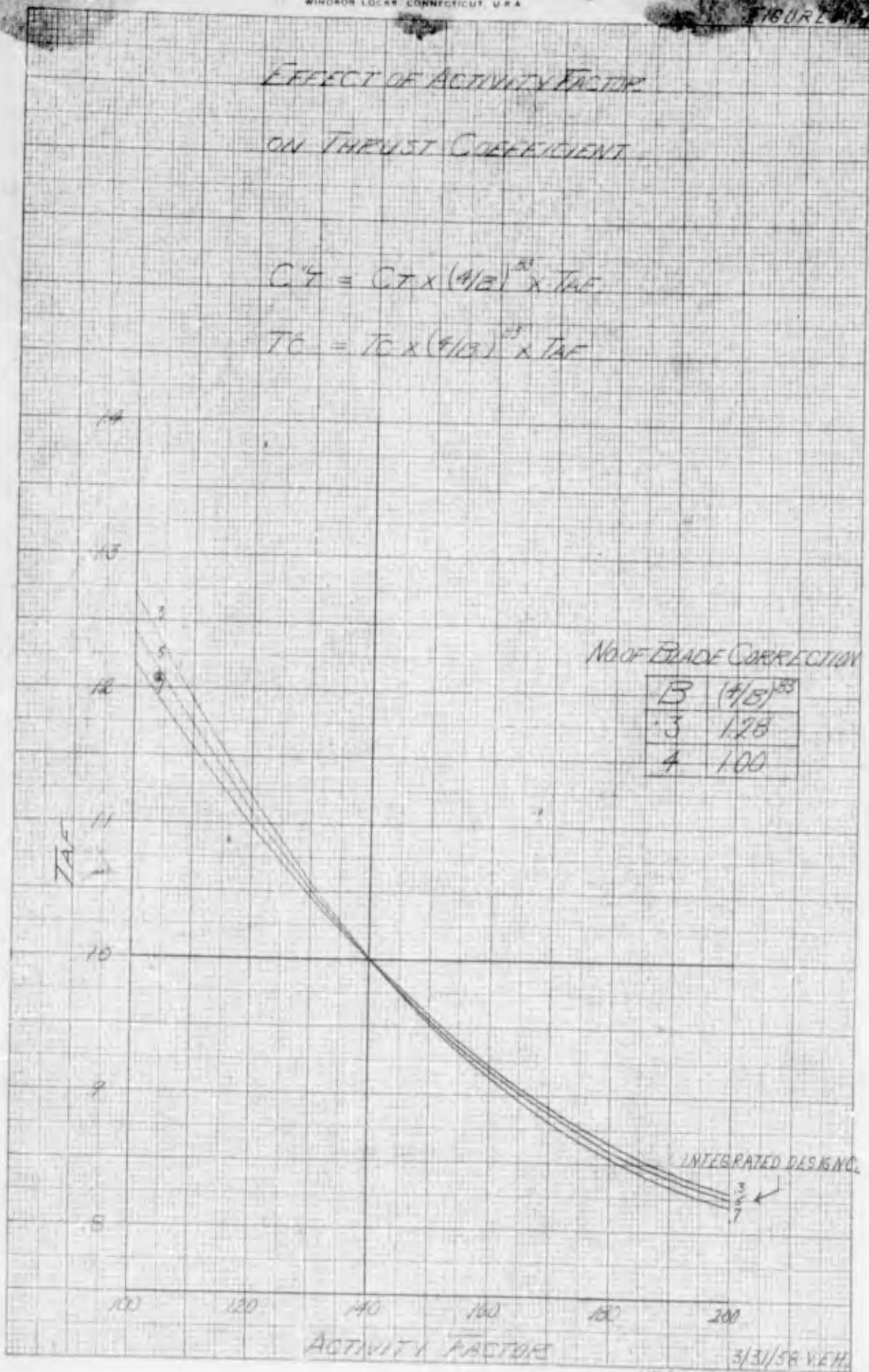

3/31/58 V.E.H.
HSD CURVE NO P-2697

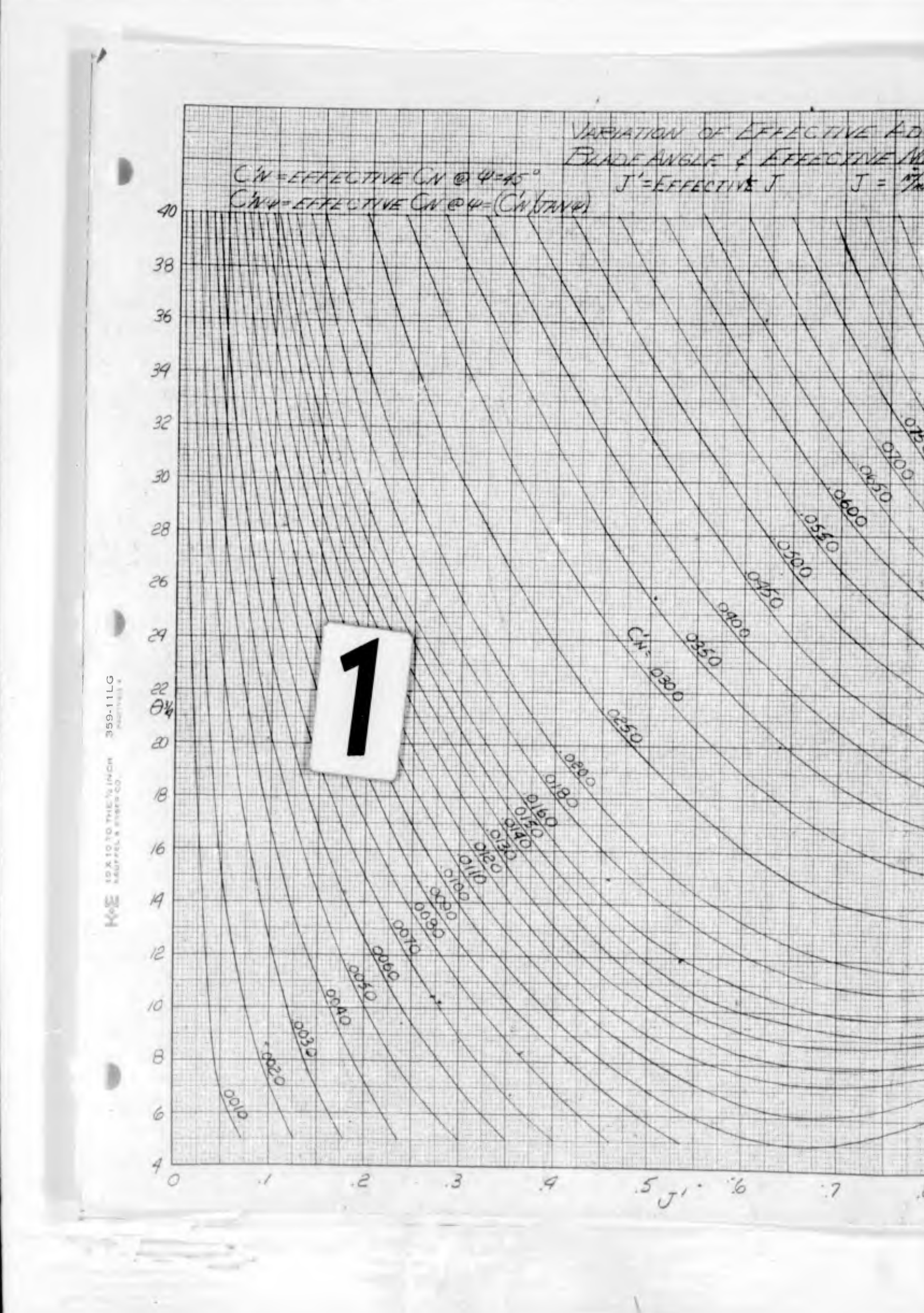
VARIATION OF EFFECTIVE AD
BLADE ANGLE & EFFECTIVE AN
C'N = EFFECTIVE CN @ Ψ=45°
C'Nψ = EFFECTIVE CN @ Ψ=(C'N)(TAN Ψ)
J' = EFFECTIVE J
J =
1
C'N=
θ¾
J'
0
.1
.2
.3
.4
.5
.6
.7
4
6
8
10
12
14
16
18
20
22
24
26
28
30
32
34
36
38
40
.0010
.0020
.0030
.0040
.0050
.0060
.0070
.0080
.0090
.0100
.0110
.0120
.0130
.0140
.0150
.0160
.0180
.0200
.0250
.0300
.0350
.0400
.0450
.0500
.0550
.0600
.0650
.0700

FIGURE A15

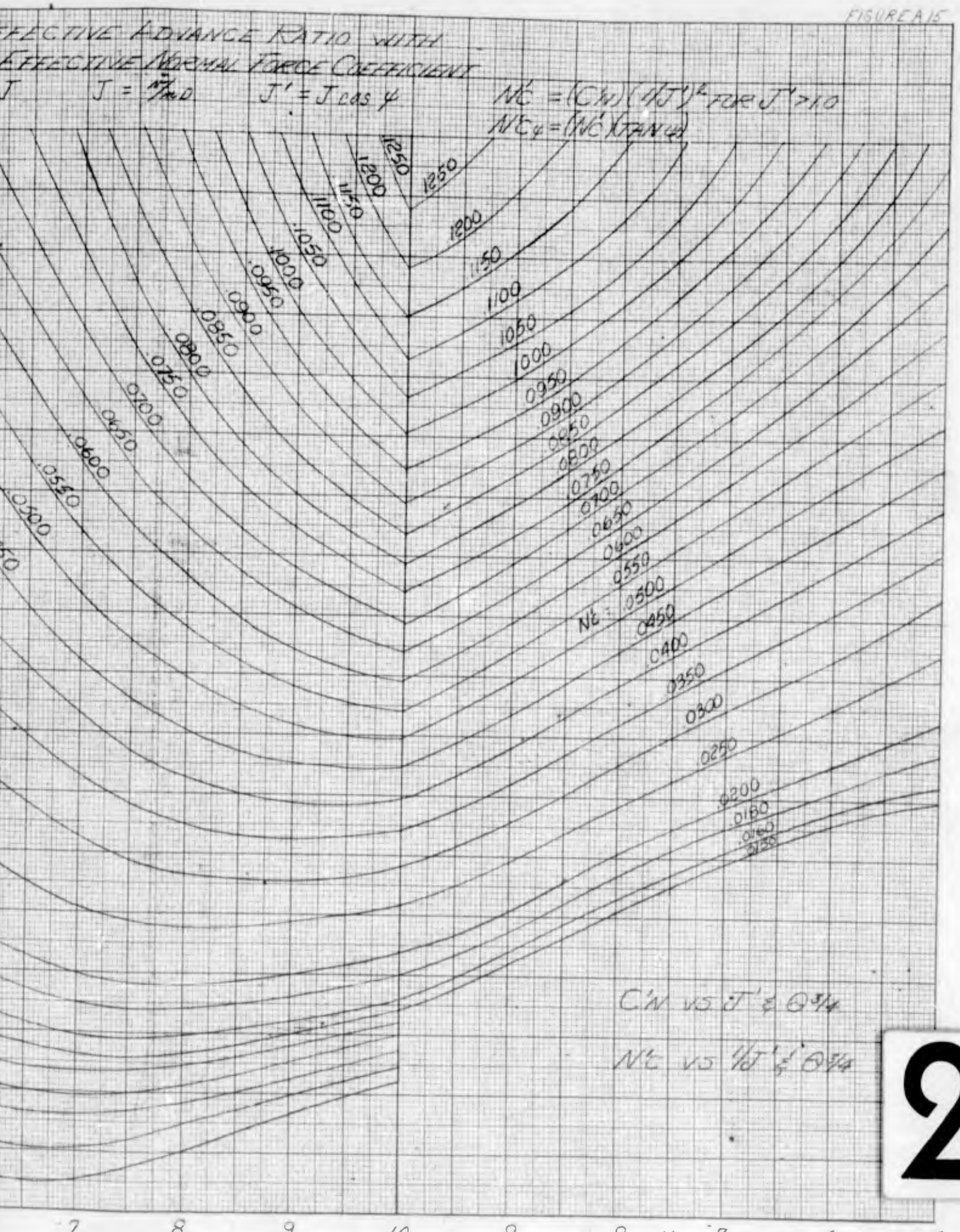
EFFECTIVE ADVANCE RATIO WITH
EFFECTIVE NORMAL FORCE COEFFICIENT
J
J = V/nD
J' = J cos ψ
NE = (CN)(1/J')² FOR J' > 1.0
NEψ = (NE)(TAN ψ)
1250
1200
1150
1100
1050
1000
0950
0900
0850
0800
0750
0700
0650
0600
0550
0500
0450
0400
0350
0300
0250
0200
0150
0100
0050
NE
.7
.8
.9
1.0
.9
.8
1/J'
.7
.6
.5
CN VS J' & Θ3/4
NE VS 1/J' & Θ3/4

2

HAMILTON STANDARD DIVISION

WINDSOR LOCKS, CONNECTICUT, U. S. A.

HS-1829

FIGURE A16

EFFECT OF INTEGRATED DESIGN C_L ON NORMAL FORCE COEFFICIENT FOR $J' \leq 1.0$

$$C''_N = C''_N - \Delta C''_N$$

$$\Delta C''_N = \left(\Delta C''_{N\,CHART}\right)\left(\frac{C_{L_d} - .300}{.200}\right)$$

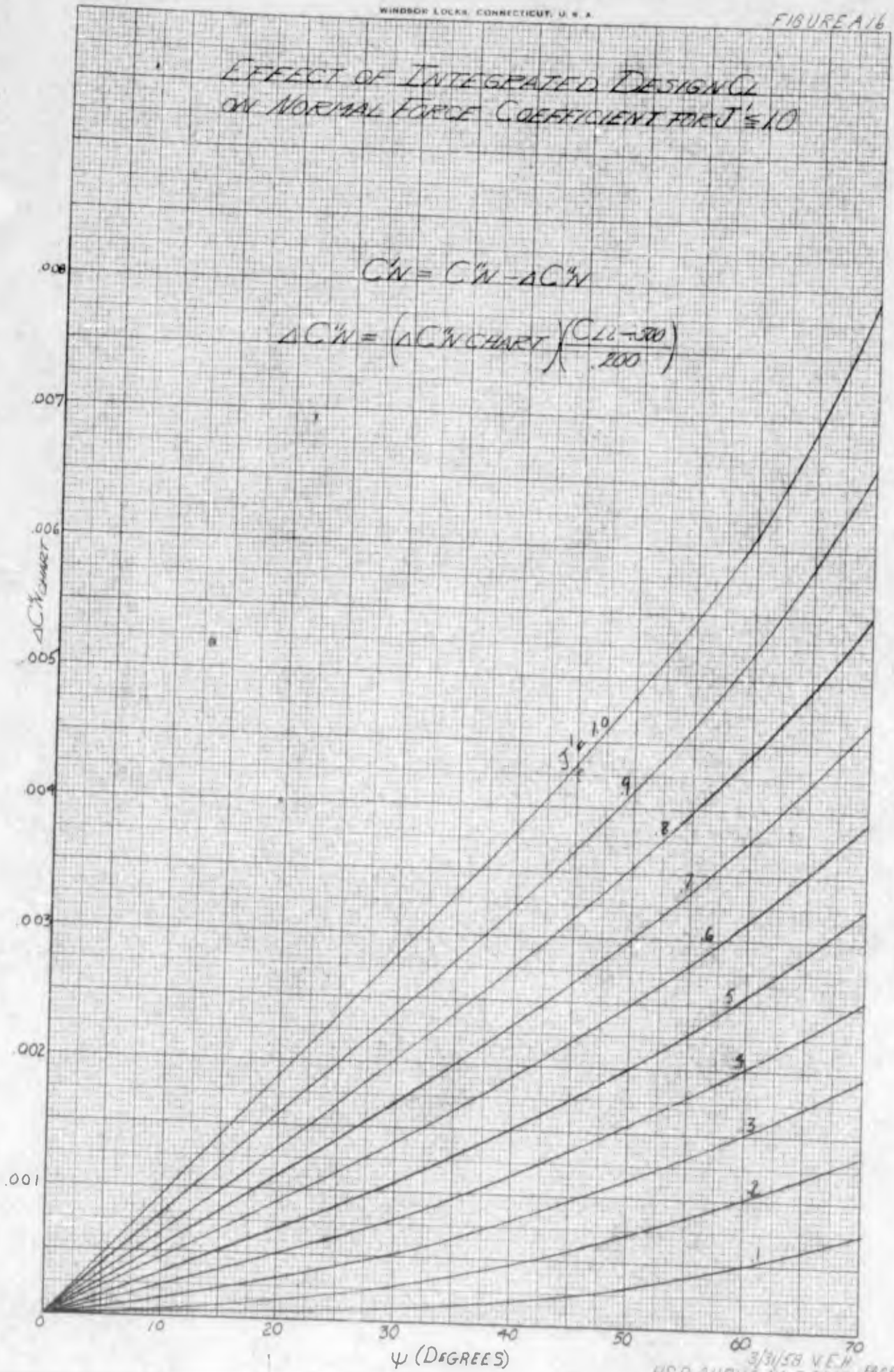

10 X 10 TO THE ½ INCH 359-11
KEUFFEL & ESSER CO.

3/31/58 V.E.H.
HSD CURVE NO. P-26296 FIGA16A1

HS P-180A -33

HAMILTON STANDARD DIVISION

WINDSOR LOCKS, CONNECTICUT, U. S. A.

65-1821

FIGURE A 17

EFFECT OF INTEGRATED DESIGN C_d ON NORMAL FORCE COEFFICIENT FOR $T_{2:0}$

$$NC' = NC - \Delta NC$$

$$\Delta NC = \left(\Delta NC \text{ CHART}\right)\left(\frac{C_{d_{2:0}}}{.200}\right)$$

ΔNC CHART

.007
.006
.005
.004
.003
.002
.001

0 10 20 30 40 50 60 70

Ψ (DEGREES)

$M = .6$
$.8$
$.9$

3/31/58 V.E.H.

HSD CURVE NO P-3-297

MADE IN U.S.A. TO THE 1/8 INCH 359-51
KEUFFEL & ESSER CO. HOBOKEN, N.J.

HS F-180A -53

HAMILTON STANDARD DIVISION

WINDSOR LOCKS, CONNECTICUT, U.S.A.

HS-1829

FIGURE A18

EFFECT OF SIDE FORCE FACTOR ON NORMAL FORCE COEFFICIENT

$$C''_N = C_N \times (4/B)^{.83} \times N_{SFF}$$

$$N_C'' = N_C \times (4/B)^{.83} \times N_{SFF}$$

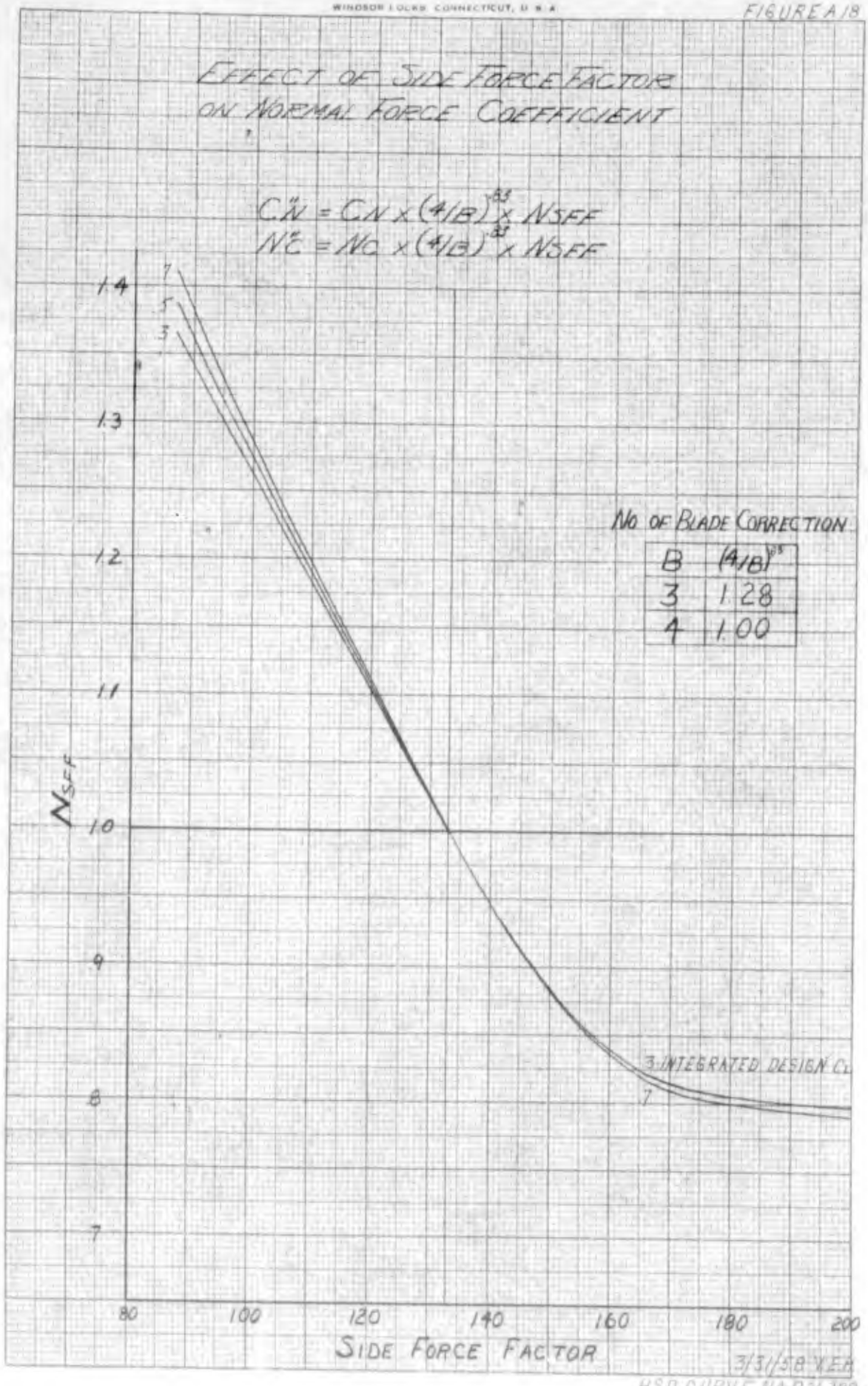

No. OF BLADE CORRECTION	
B	$(4/B)^{.83}$
3	1.28
4	1.00

3/31/58 V.E.R.

HSD CURVE NO R26298

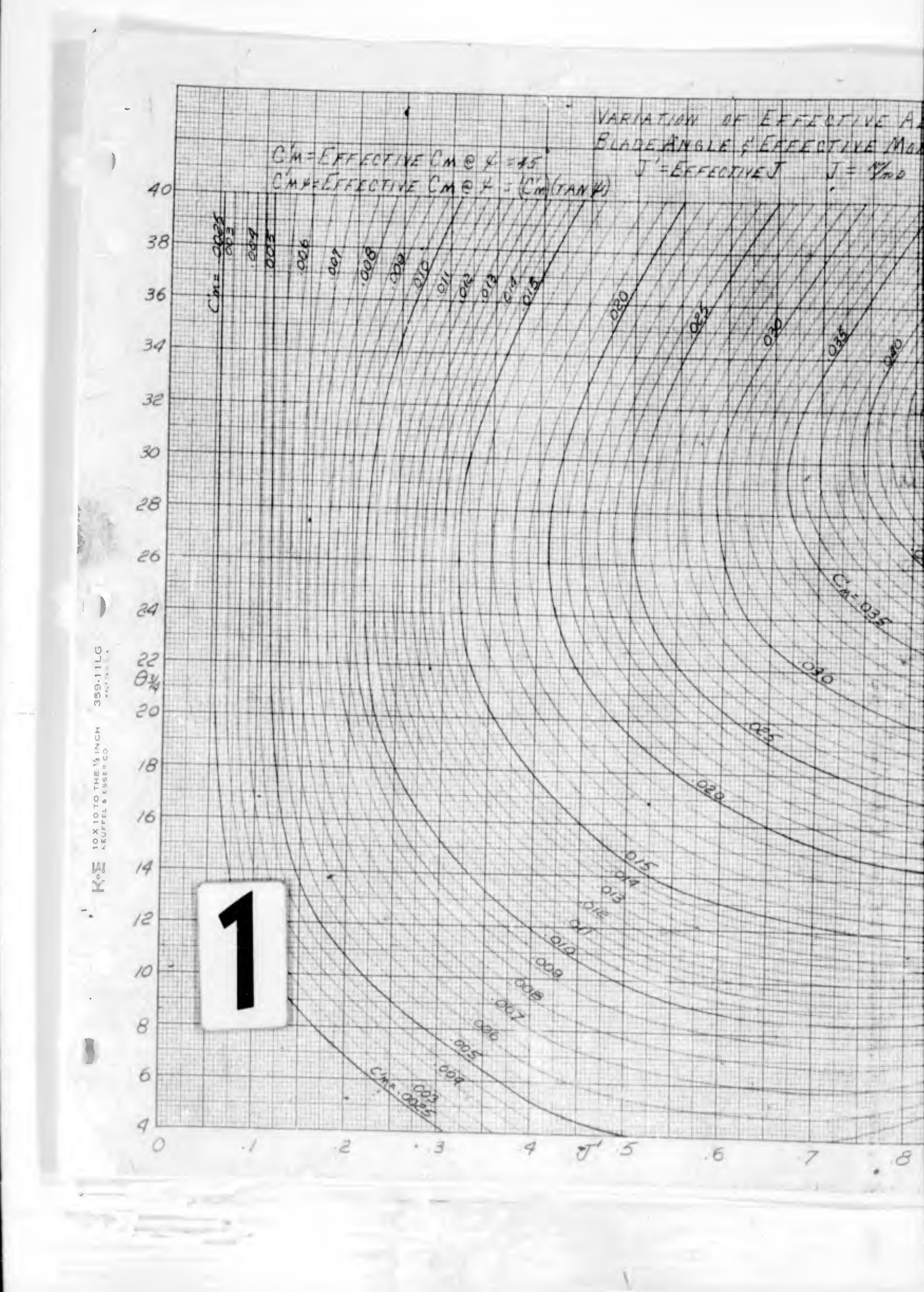
VARIATION OF EFFECTIVE A
BLADE ANGLE & EFFECTIVE MO
J' = EFFECTIVE J
C'M = EFFECTIVE CM @ ϕ = 45
C'M = EFFECTIVE CM @ ϕ = (C'M)(TAN ϕ)
CM = .0025
.002
.004
.005
.006
.007
.008
.009
.010
.011
.012
.013
.014
.015
.020
.025
.030
.035
.040
CM = .035
.030
.025
.020
.015
.014
.013
.012
.011
.010
.009
.008
.007
.006
.005
.004
.003
CM = .0025
θ3/4
J'
0
.1
.2
.3
.4
.5
.6
.7
.8
4
6
8
10
12
14
16
18
20
22
24
26
28
30
32
34
36
38
40
1
359-11LG
10 X 10 TO THE ½ INCH
KEUFFEL & ESSER CO

AS-1824

FIGURE A 19

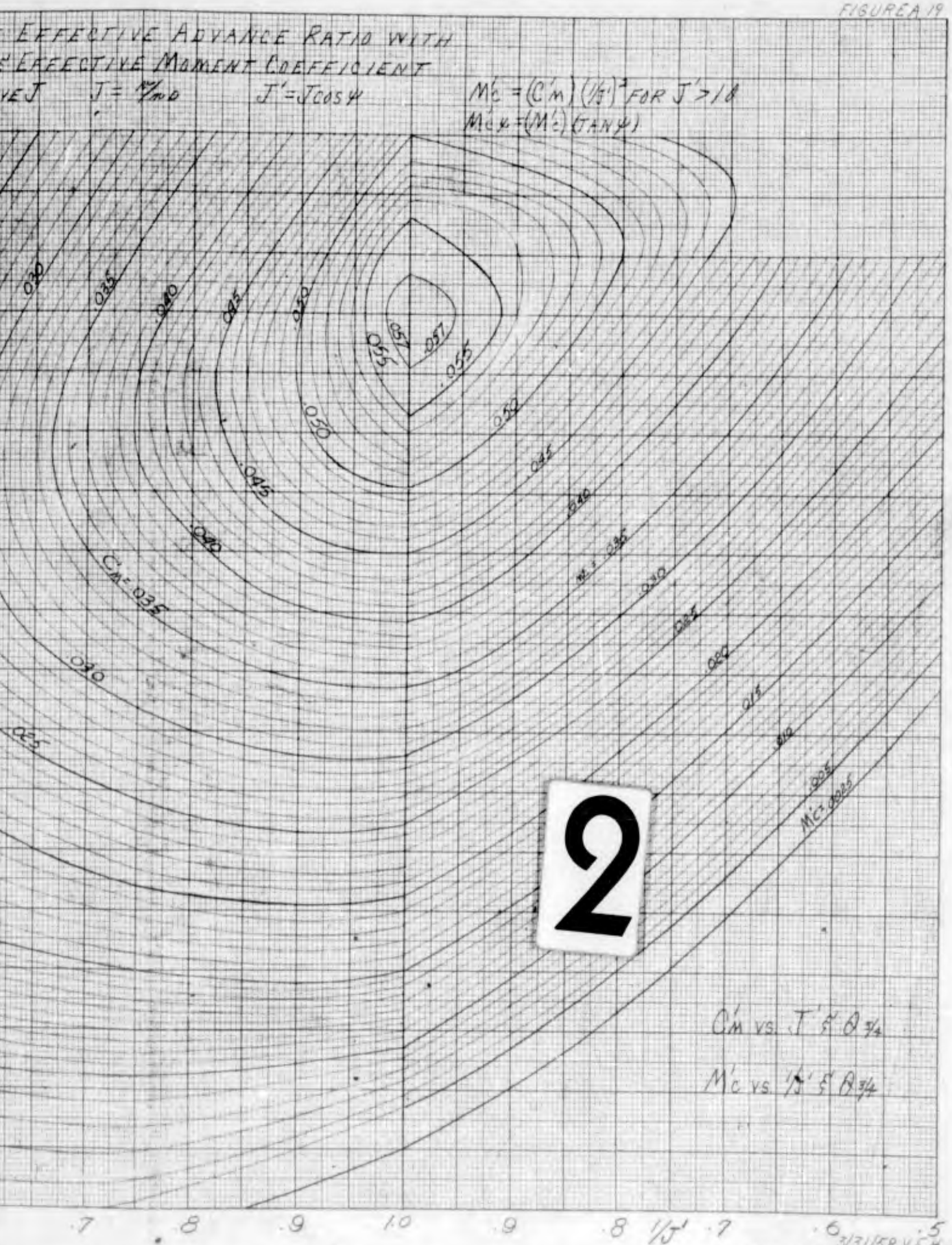

3/31/58 V.E.M.
HSD CURVE NO P-2699 PAGE A-19

FIGURE A-20

HAMILTON STANDARD DIVISION

WINDSOR LOCKS, CONNECTICUT, U. S. A.

EFFECT OF INTEGRATED DESIGN C_L ON MOMENT COEFFICIENT FOR $J' \leq 1.0$

$$C'_M = C''_M - \Delta C''_M$$

$$\Delta C''_M = \left(\Delta C''_M \text{ CHART}\right)\left(\frac{C_L - .500}{.200}\right)$$

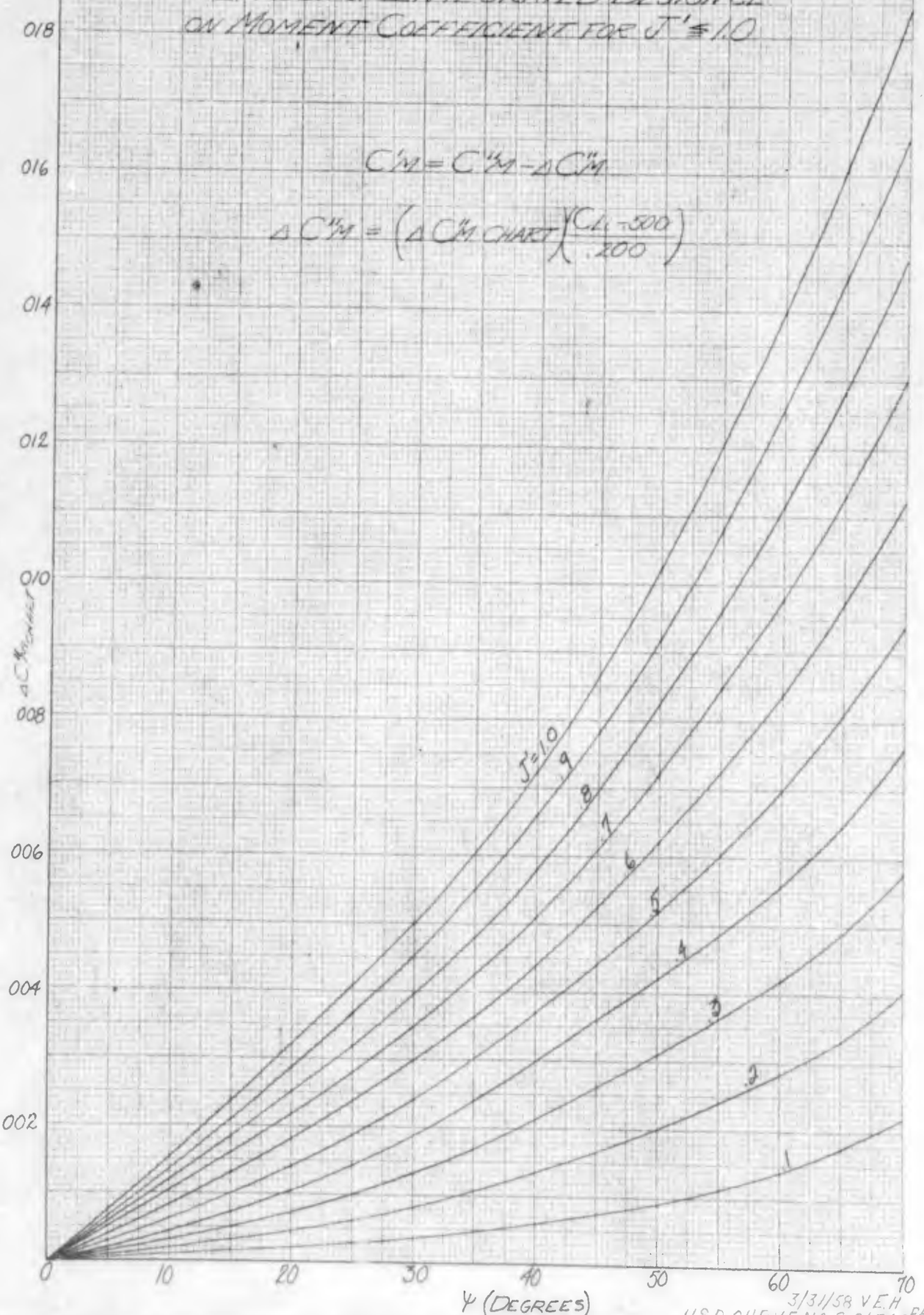

3/31/58 V.E.H

HSD CURVE NO P-26300 PAGE 1

FIGURE A 21

HAMILTON STANDARD DIVISION

WINDSOR LOCKS, CONNECTICUT, U. S. A.

EFFECT OF INTEGRATED DESIGN C_L ON MOMENT COEFFICIENT FOR $J' \geq 1.0$

$$M_C = M_C'' - \Delta M_C''$$

$$\Delta M_C'' = \left(\Delta M_{C\,CHART}\right)\left(\frac{C_{L_D} \div .500}{.200}\right)$$

$\Delta M_{C\,CHART}$

018
016
014
012
010
008
006
004
002

$K_J = 1.0$
9
8
7
6
5

0 10 20 30 40 50 60 70

Ψ (DEGREES)

3/31/59 V.E.H.
HSD CURVE NO. C-21-2A | PAGE 46

HAMILTON STANDARD

WINDSOR LOCKS, CONNECTICUT, U.S.A.

HS-1829

FIGURE A 22

EFFECT OF ACTIVITY FACTOR ON MOMENT COEFFICIENT

$$C_M'' = C_M \times (4/B)^{.33} \times MAF$$

$$M_C'' = M_C \times (4/B)^{.33} \times MAF$$

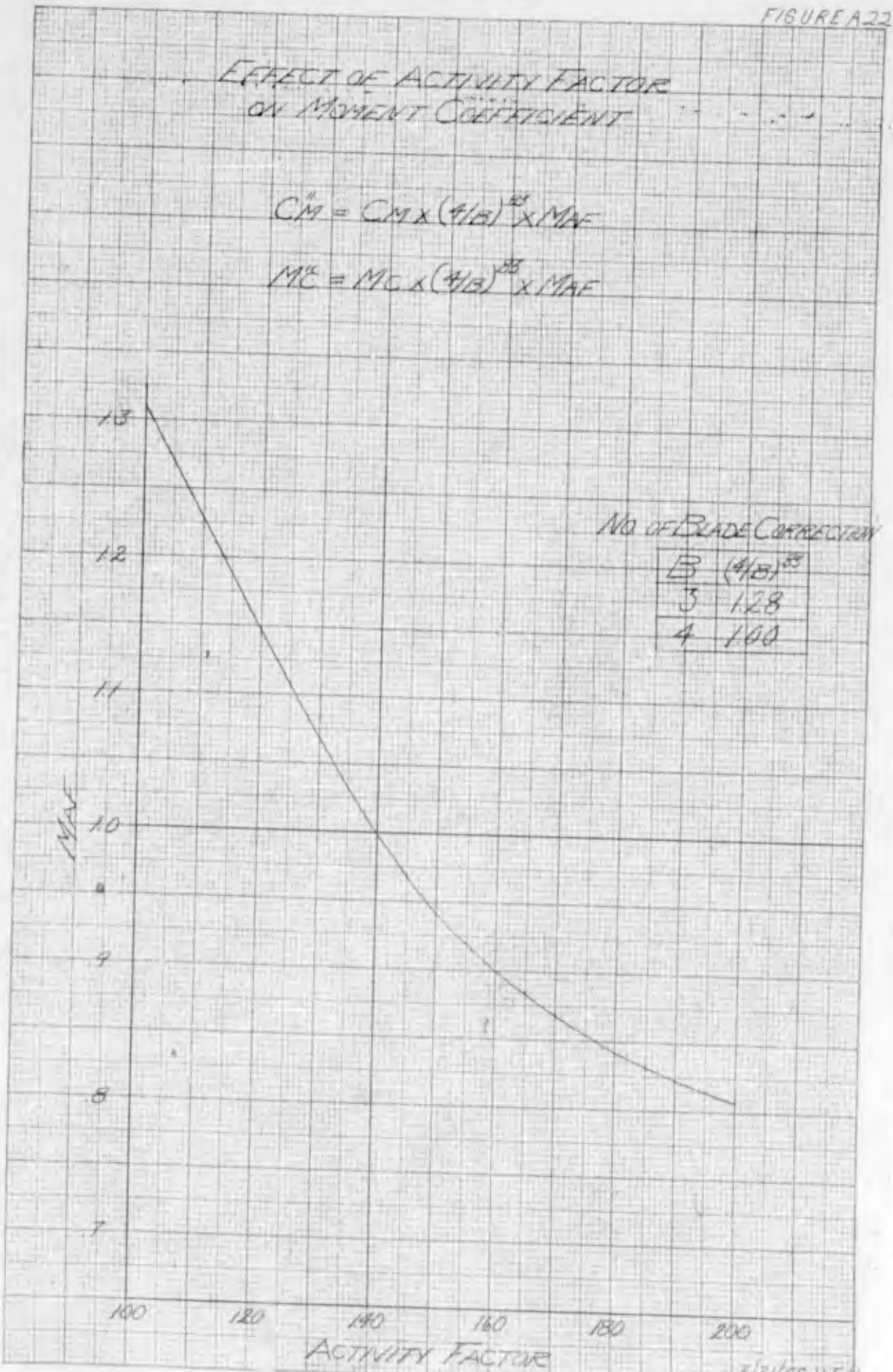

No. of Blade Correction

B	$(4/B)^{.33}$
3	1.28
4	1.00

3/31/58 V.E.H

HSD CURVE NO. PJ6302

APPENDIX B

PROPELLER EFFICIENCY CHARTS AND THEIR USE

Included in this appendix is a set of six propeller efficiency charts of the following propeller configurations:

Figure	Number of Blades	Activity Factor	Integrated Design C_L
B1	4	140	0.300
B2	4	"	0.500
B3	4	"	0.700
B4	3	"	0.300
B5	3	"	0.500
B6	3	"	0.700

These charts are included to facilitate the choice of a propeller when considering only the steady state (or unskewed) conditions. In using these charts, the only variable that is involved is blade Activity Factor, which may easily be corrected by use of the Activity Factor to Torque coefficient (Fig. A1) which is included in this appendix as Fig. B-7.

Therefore, C_{PE} or chart value of $C_p = C_p \times Q_{AF}$. By plotting values of efficiency against values of Integrated Design C_L for a given Activity Factor blade, the propeller selection becomes an easy one. This is illustrated on Fig. B8.

The compressibility correction is handled separately in Appendix C.

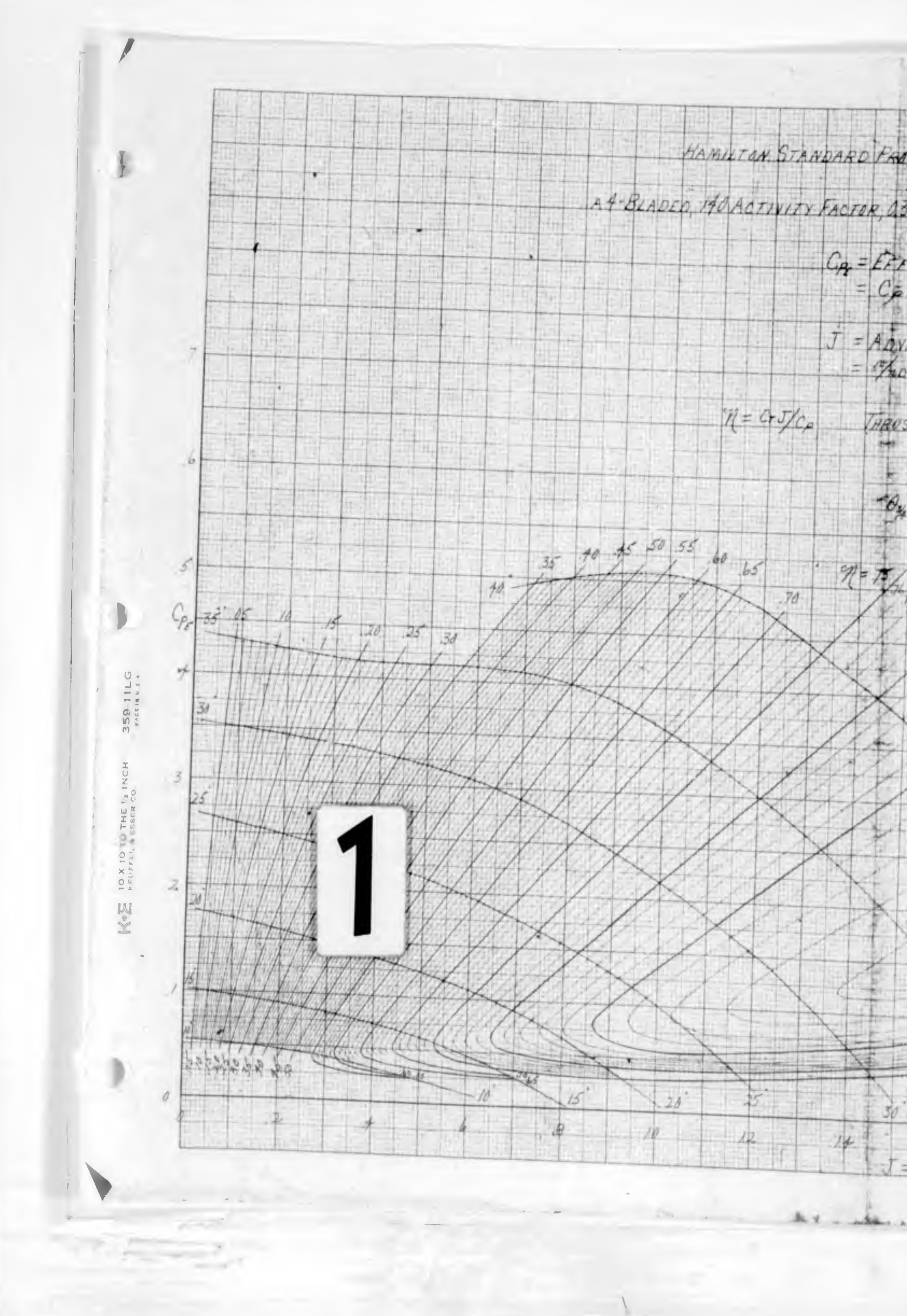
HAMILTON STANDARD PRO
4-BLADED, 140 ACTIVITY FACTOR, 0.3
C_{P_c} = EFF
= C_P
J = ADV
= V/nD
η = C_TJ/C_P
THRUS
$\theta_{.75}$
C_{P_c}
35° 40 45 50 55 60 65 70
10 15 20 25 30
J =
1
K&E 10 X 10 TO THE 1/2 INCH 359-11LG
KEUFFEL & ESSER CO. MADE IN U.S.A.

FIGURE B-1

...ILTON STANDARD PROPELLER EFFICIENCY CHART

FOR

...0 ACTIVITY FACTOR, 0.300 INTEGRATED DESIGN C_L PROPELLER

4/140 AF/.300 C_{L_i}

C_{P_t} = EFFECTIVE C_P
= $C_P \times Q_{AF}$

J = ADVANCE RATIO
= V_K/n_D = $1014\, V_K/ND$

$\eta = C_T J / C_P$ $\quad$ THRUST = $\frac{326\, BHP\, \eta}{V_K}$ (POUNDS)

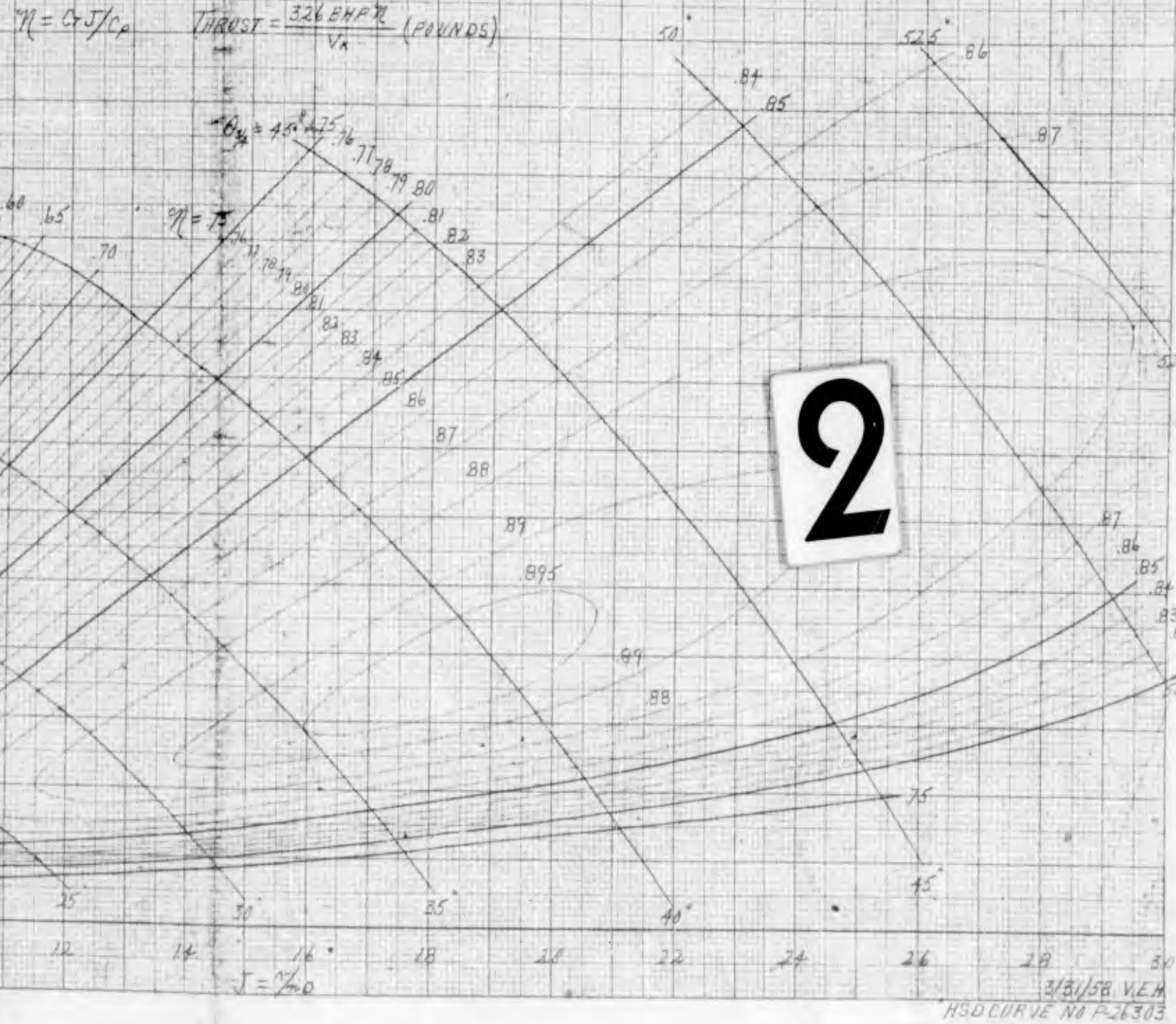

2

3/31/58 V.E.M.

HSD CURVE NO P-26303

FIGURE B1

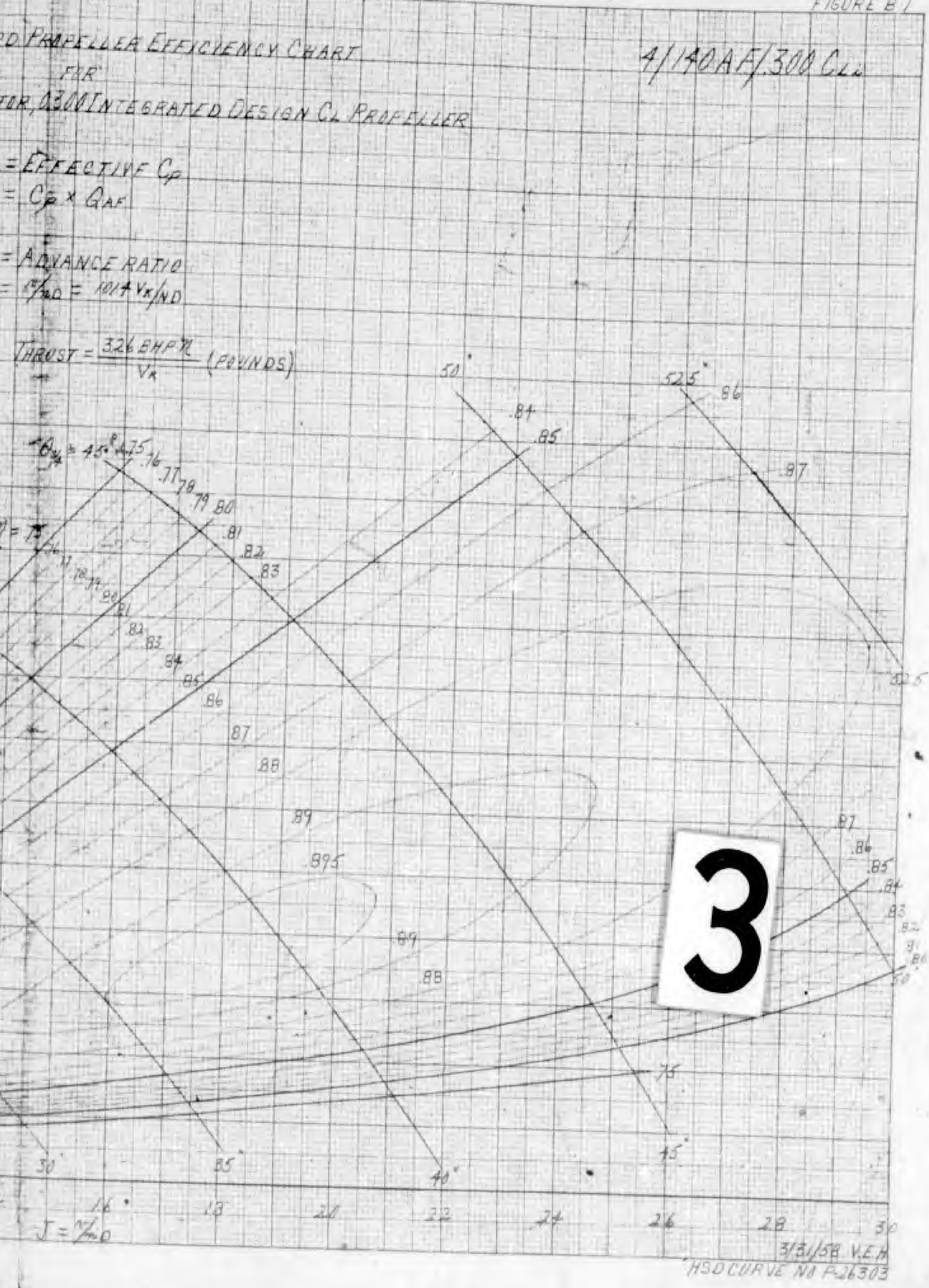
...D PROPELLER EFFICIENCY CHART
FOR
...TOR, 0.300 INTEGRATED DESIGN CL PROPELLER
4/140AF/.300 CLi
= EFFECTIVE Cp
= Cp × QAF
= ADVANCE RATIO
= V/nD = 101.4 VK/ND
THRUST = 326 BHP η / VK (POUNDS)
J = V/nD
3/31/58 V.E.H
HSD CURVE NO P-26303

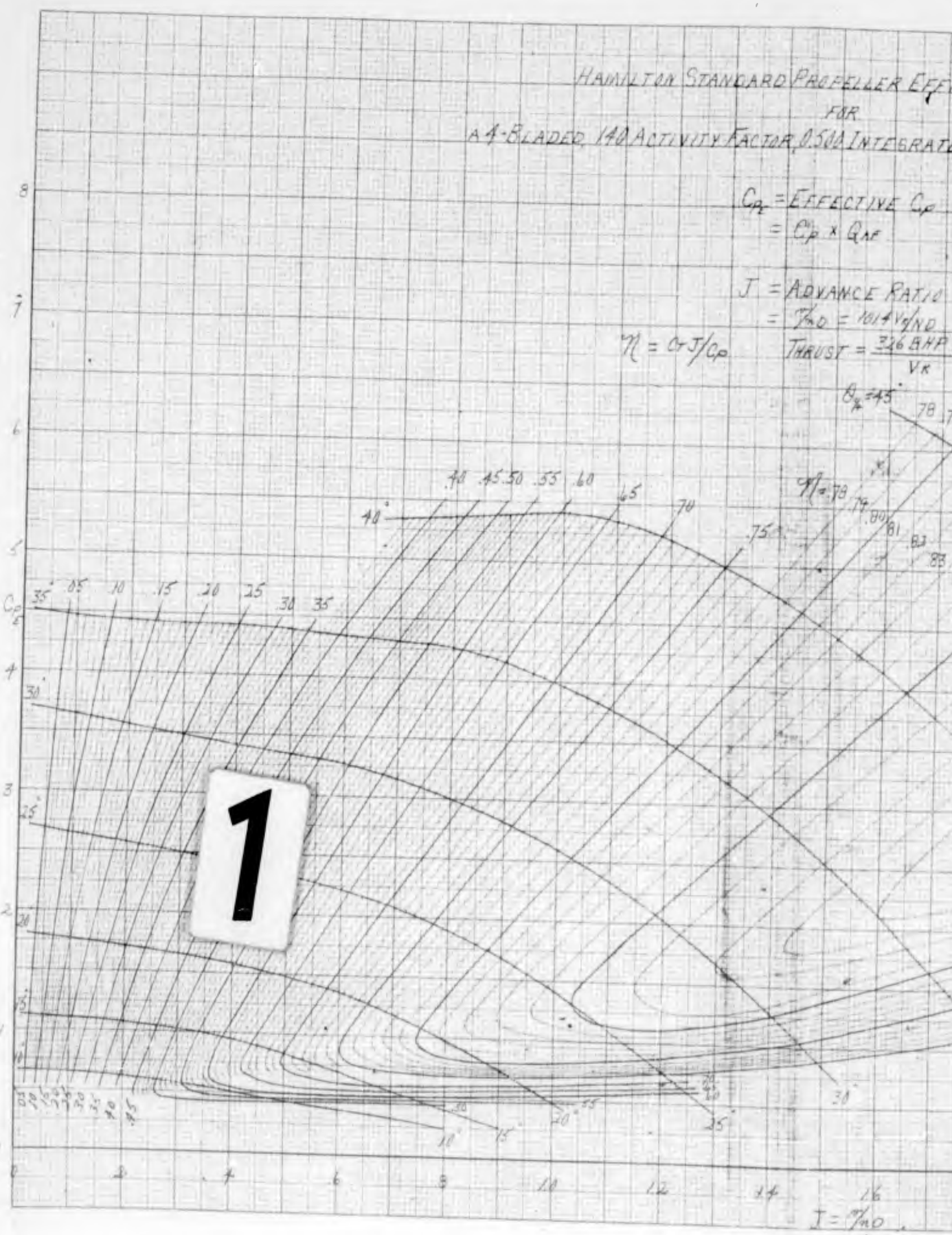

FIGURE B 2

STANDARD PROPELLER EFFICIENCY CHART-
FOR
VITY FACTOR, 0.500 INTEGRATED DESIGN C_L PROPELLER

4/140 AF/.508 C_{L_i}

C_P = EFFECTIVE C_p
= $C_p \times Q_{AF}$

J = ADVANCE RATIO
= $\frac{V_K}{ND} = 1014 \frac{V_K}{ND}$

$\frac{J}{C_P}$ THRUST = $\frac{326\ BHP\ \eta}{V_K}$ (POUNDS)

$\theta_{.75} = 45°$

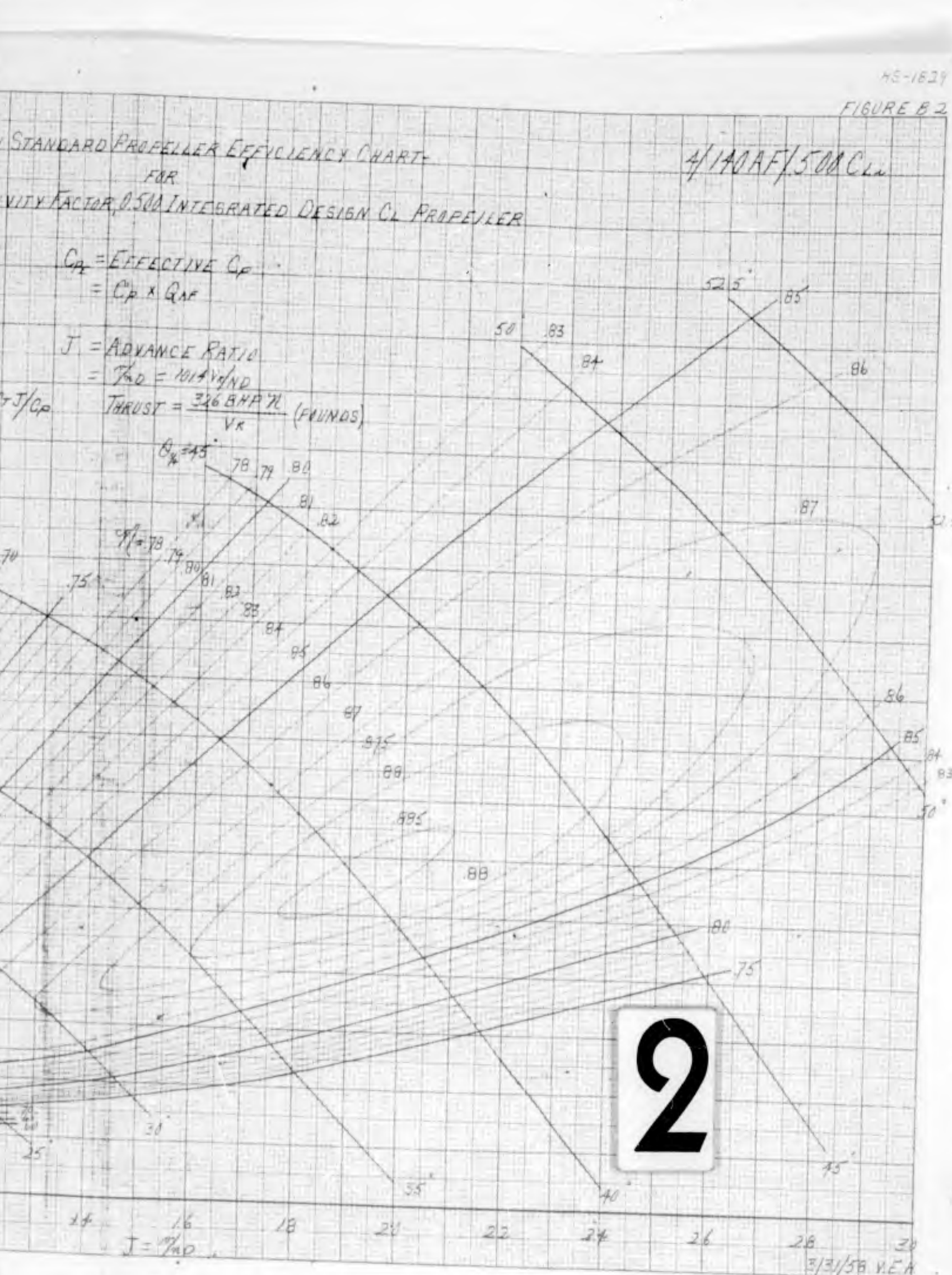

3/31/56 V.E.A
HSD CURVE NO P26304

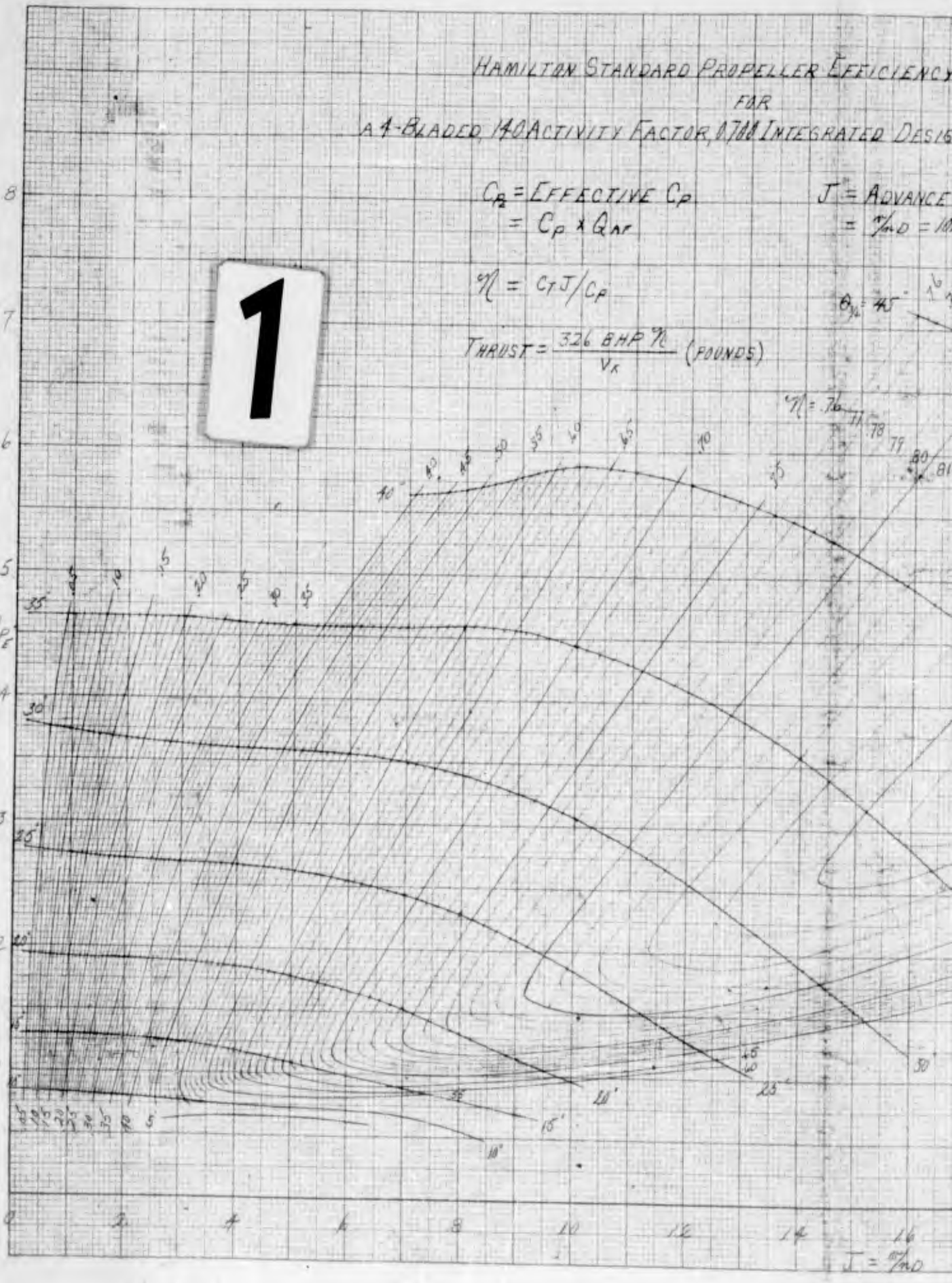
HAMILTON STANDARD PROPELLER EFFICIENCY
FOR
A 4-BLADED, 140 ACTIVITY FACTOR, 0.700 INTEGRATED DESIG
C_{P_E} = EFFECTIVE C_P
= $C_P \times Q_{AF}$
J = ADVANCE
= V/nD = 10
$\eta = C_T J / C_P$
$\theta_{.75}$ = 45°
THRUST = $\frac{326\ BHP\ \eta}{V_K}$ (POUNDS)
η = .76 .78 .79 .80 .81
C_{P_E}
J = V/nD
1
10 X 10 TO THE ½ INCH
KEUFFEL & ESSER CO.
359-11LG
MADE IN U.S.A.

FIGURE B 8

PELLER EFFICIENCY CHART
TAR
ID INTEGRATED DESIGN CL PROPELLER

J = ADVANCE RATIO
$= V_A/nD = 101.4 V_K/ND$

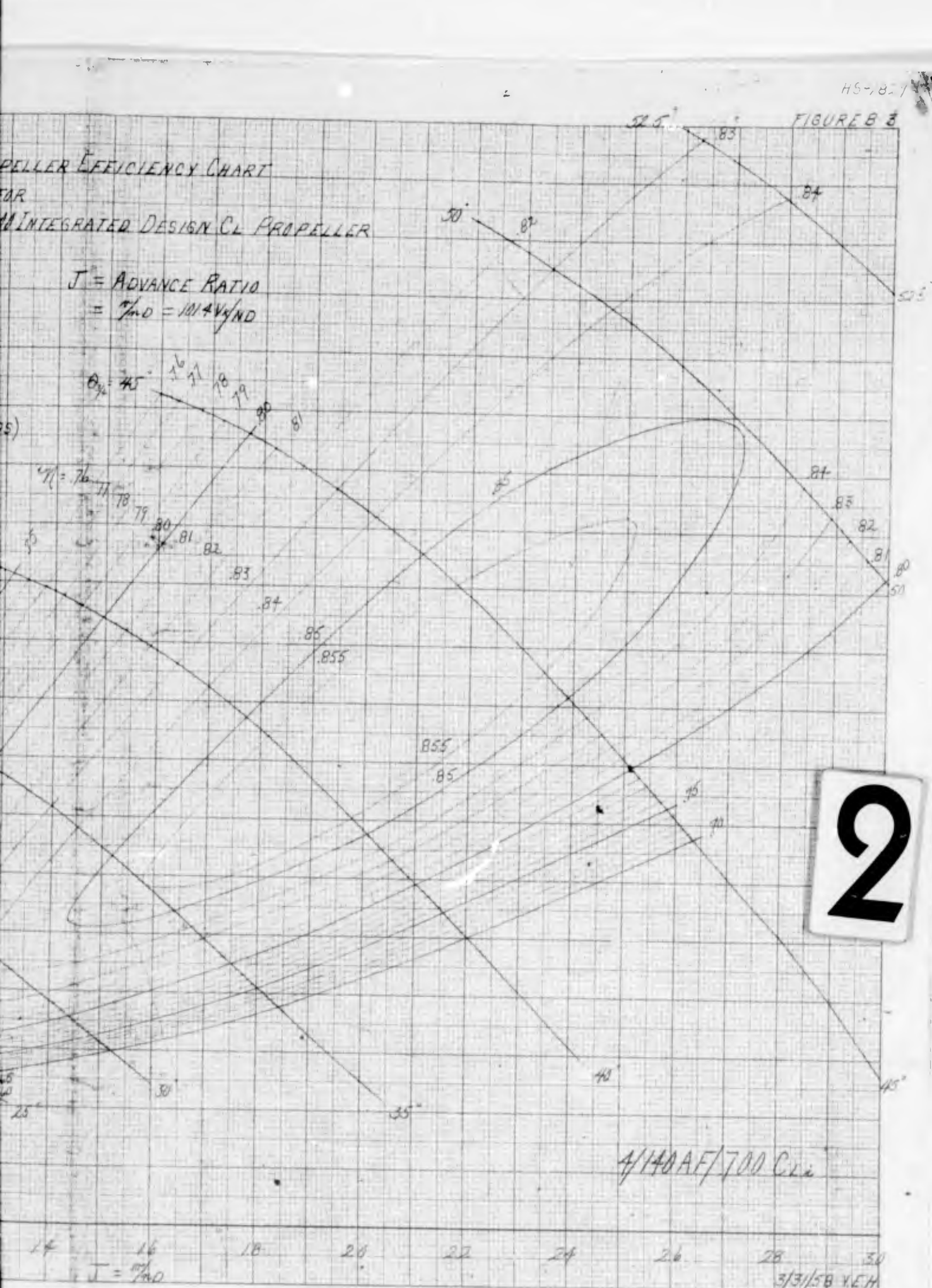

4/140AF/700 CLi

3/31/58 V.E.H.
HSD CURVE NO P-26305

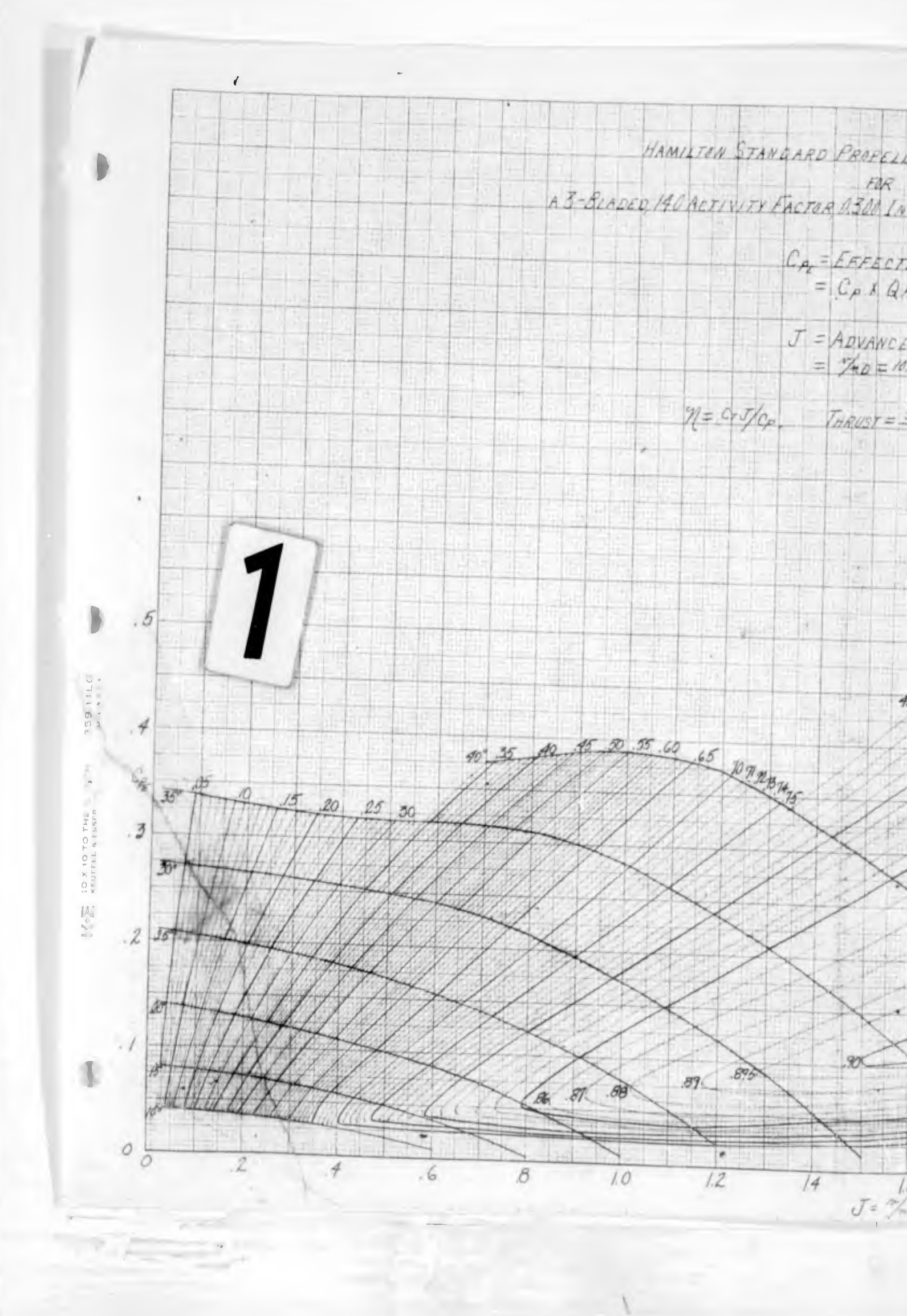
HAMILTON STANDARD PROPELL
FOR
A 3-BLADED 140 ACTIVITY FACTOR 9.300 I
C_{P_E} = EFFECT
= C_P x Q
J = ADVANCE
= V/nD = 10
η = C_T J/C_P THRUST =
1
.5
.4
.3
.2
.1
0
0
.2
.4
.6
.8
1.0
1.2
1.4
J = V/
40°
35
40
45
50
55
60
65
35°
05
10
15
20
25
30
30°
25°
20°
15°
10°
.80
.87
.88
.89
.895
10 X 10 TO THE
KEUFFEL & ESSER

AS-1829

FIGURE B 4

STANDARD PROPELLER EFFICIENCY CHART — 3/140AF.300 C_{L_i}

FOR

ITY FACTOR 0.300 INTEGRATED DESIGN C_L PROPELLER

C_{P_L} = EFFECTIVE C_P

$= C_P \times Q_{AF}$

J = ADVANCE RATIO

$= V_K/ND = 1014\, V_K/ND$

J/C_P. THRUST $= \frac{326\, BHP\, \eta}{V_K}$ (POUNDS)

2

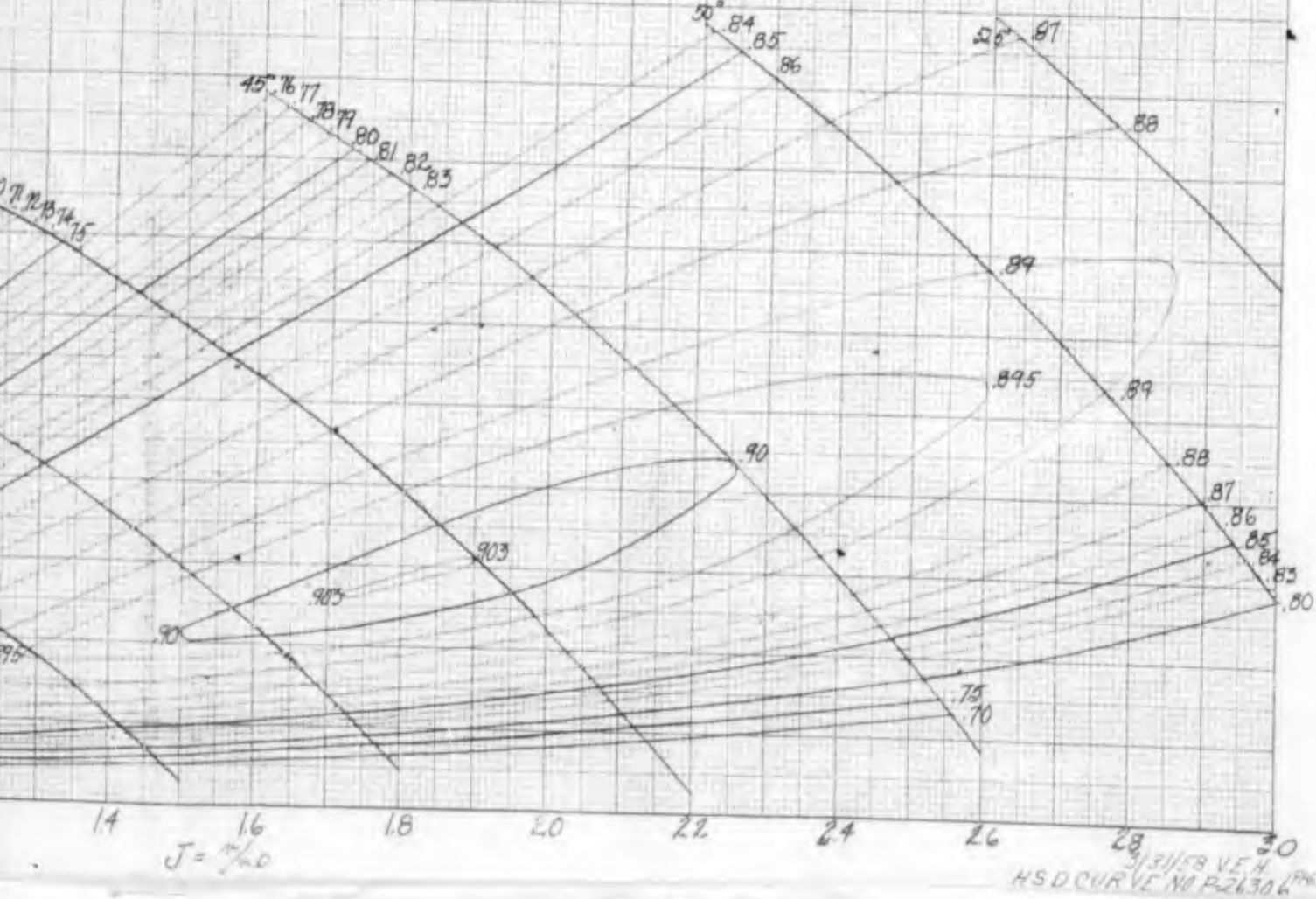

3/31/58 V.E.H.

HSD CURVE NO P-26306 (P6652)

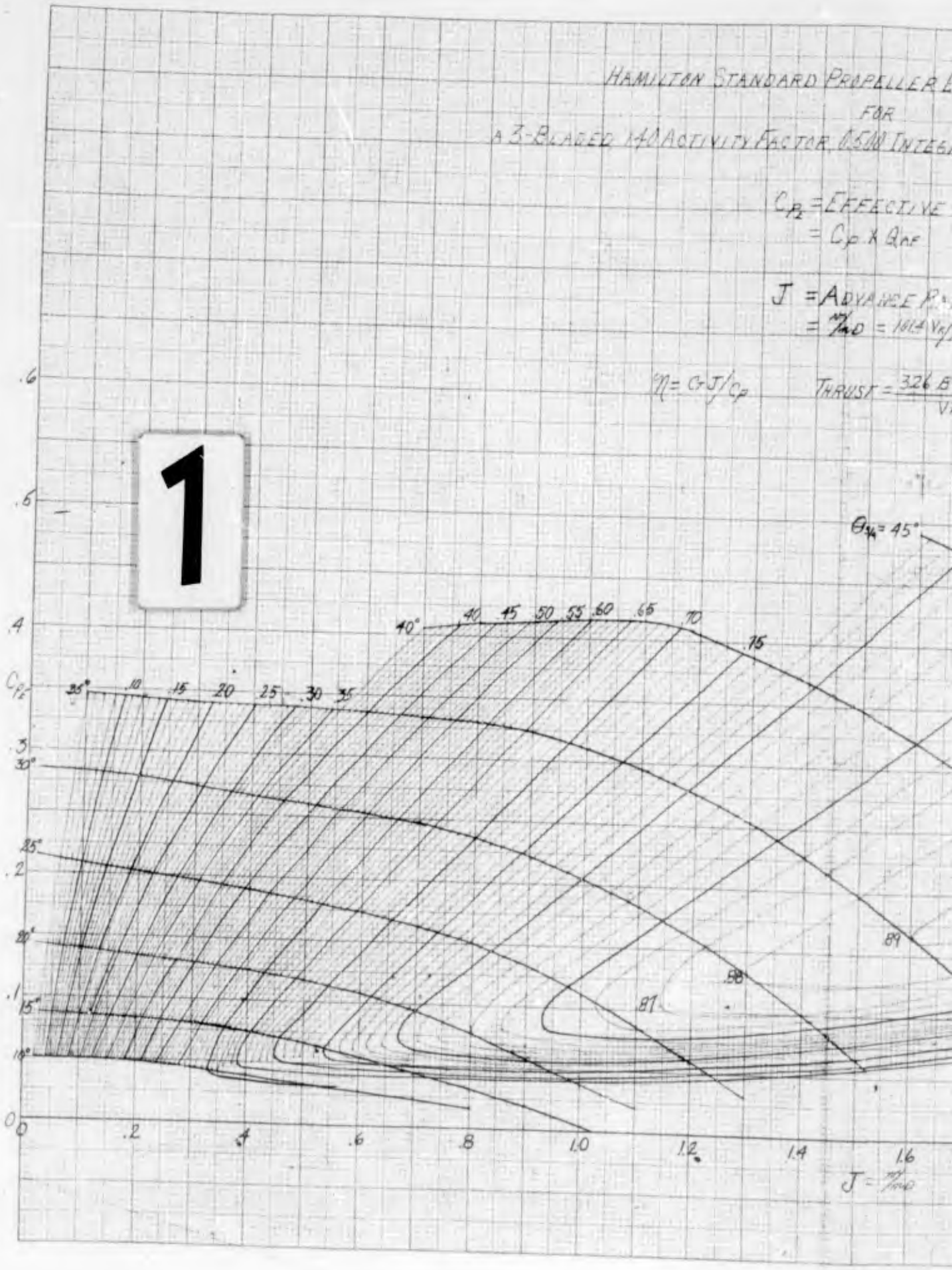

FIGURE E 5

NDARD PROPELLER EFFICIENCY CHART
FOR
FACTOR, 0.500 INTEGRATED DESIGN CL PROPELLER

3/140AE/500 CL

C_{P_E} = EFFECTIVE C_p
= $C_p \times Q_{HF}$

J = ADVANCE RATIO
= $\frac{V_K}{ND}$ = 101.4 V_K/ND

THRUST = $\frac{326\ BHP\ \eta}{V_K}$ (POUNDS

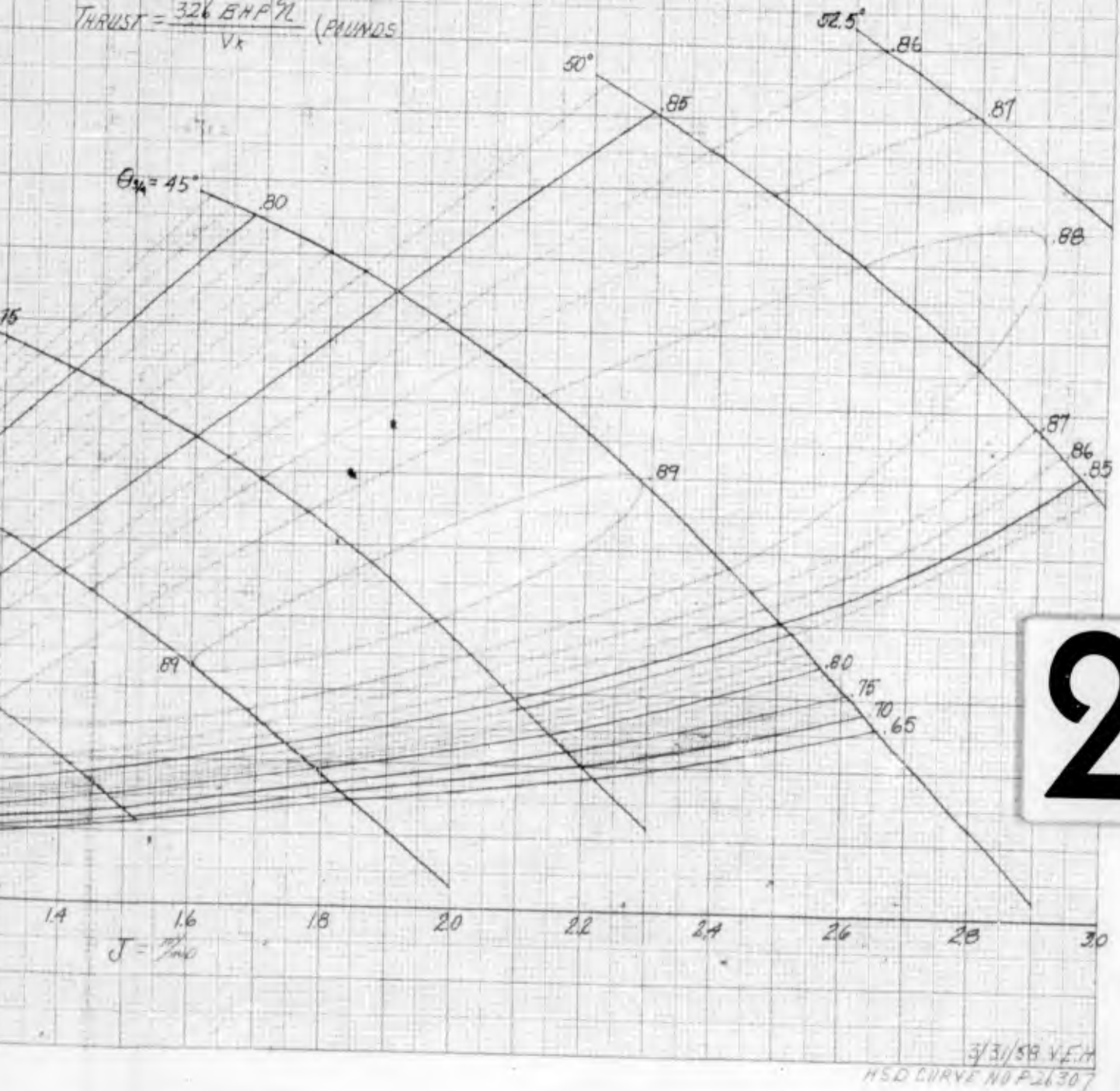

3/31/58 V.E.H
HSD CURVE NO P 26307

2

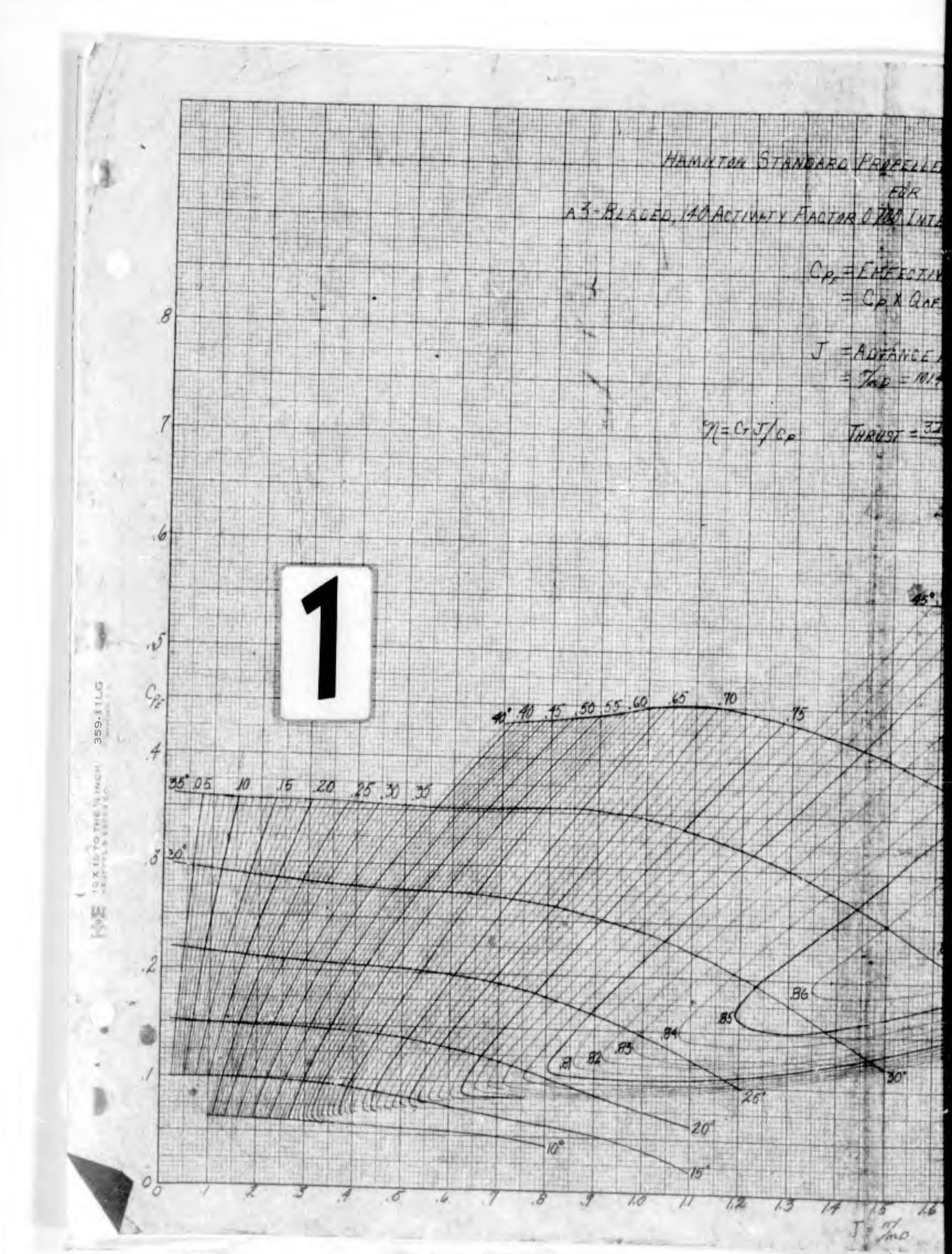
HAMILTON STANDARD PROPELLE
FOR
A 3-BLADED, 140 ACTIVITY FACTOR
C_{P_c} = EFFECTIV
= C_P X
J = ADVANCE
= V_{AD} =
$\eta = C_T J / C_P$
THRUST =
1
C_{P_c}
$J = \frac{V}{nD}$
35° .05 .10 .15 .20 .25 .30 .35
40° .40 .45 .50 .55 .60 .65 .70 .75
45°
30°
26°
20°
15°
10°
B1 B2 B3 B4 B5 B6
0 .1 .2 .3 .4 .5 .6 .7 .8
0 .1 .2 .3 .4 .5 .6 .7 .8 .9 1.0 1.1 1.2 1.3 1.4 1.5 1.6

HS-1829

FIGURE B 6

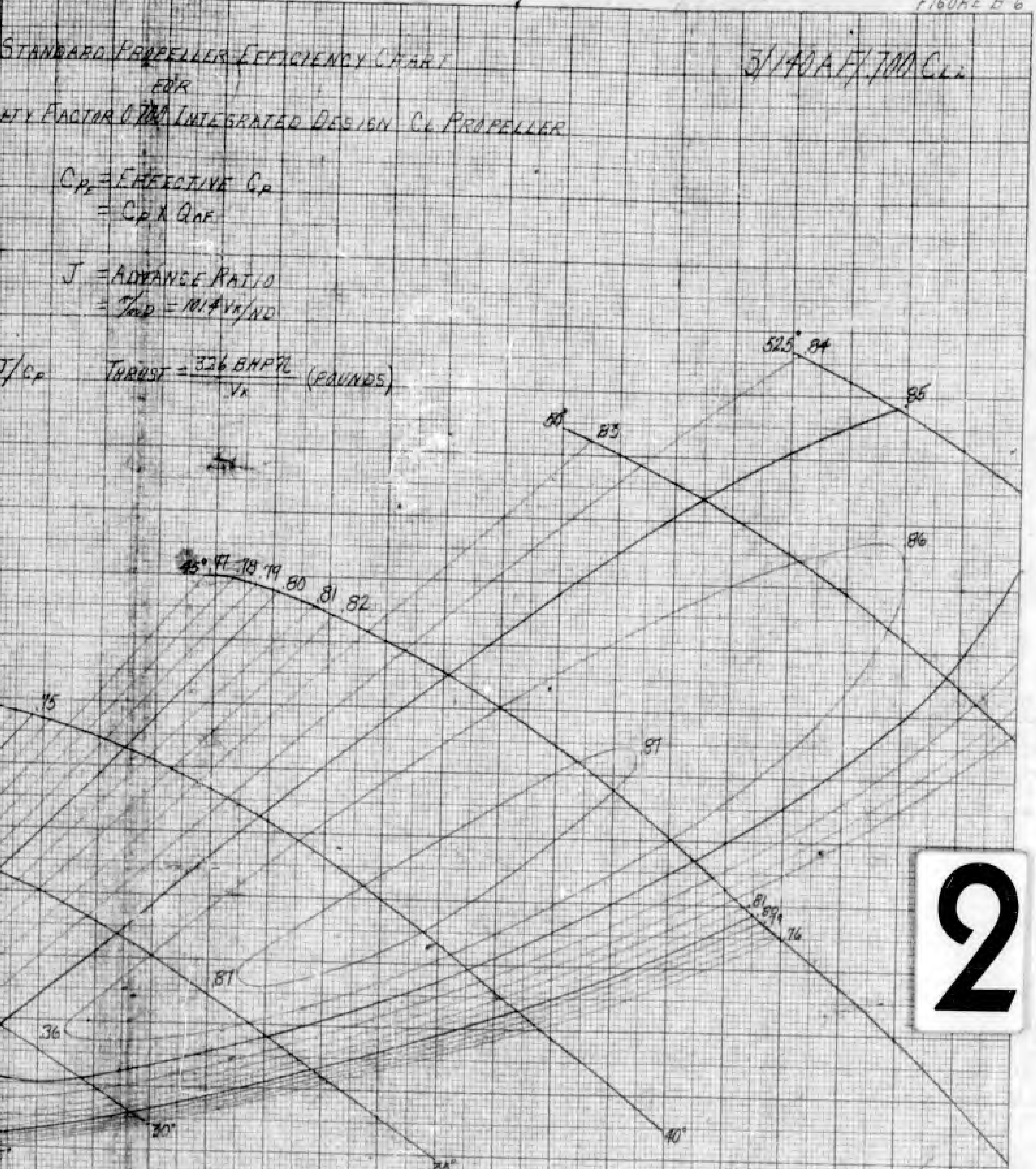

3/31/58 V.E.H.

HSD CURVE NO. P-26308

HAMILTON STANDARD DIVISION
WINDSOR LOCKS, CONNECTICUT, U. S. A.

SAMPLE PROBLEM

GIVEN: PROPELLER A: 4 BLADES, 140 AF
PROPELLER B: 4 BLADES, 170 AF
CONDITION 1: J = 0.60, Cp = 0.300
CONDITION 2: J = 1.10, Cp = 0.130

PROBLEM: WHAT C_{Li} IS REQUIRED TO GIVE AN η OF 0.80 FOR CONDITION 2 & WHICH PROPELLER HAS THE BEST PERFORMANCE FOR CONDITION 2.

	BLADE	A →			B →		
	AF	170 →			140 →		
	C_{Li}	0.300	0.500	0.700	0.300	0.500	0.700
	Q_{AF}	0.879	0.870	0.860	1.0	1.0	1.0
	FIG.	B1	B2	B3	B1	B2	B3
CONDITION 1	J	0.60 →					
	C_P	0.300 →					
	C_{PE}	0.264	0.261	0.258	0.300	0.300	0.300
	η	0.558	0.601	0.620	0.518	0.568	0.591
CONDITION 2	J	1.10 →					
	C_P	0.130 →					
	C_{PE}	0.114	0.113	0.112	0.130	0.130	0.130
	η	0.872	0.850	0.880	0.868	0.859	0.752

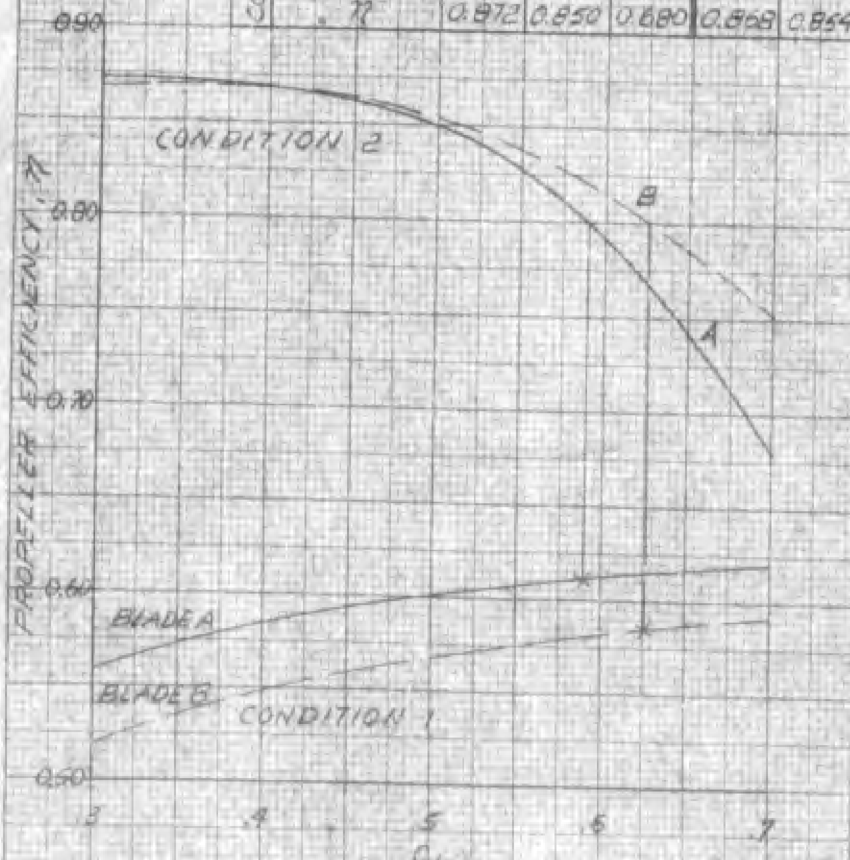

BLADE A REQUIRES A C_{Li} OF 0.590 TO GET AN EFFICIENCY OF 0.800 FOR CONDITION 2 & HAS AN EFFICIENCY OF 0.610 FOR CONDITION 1.

BLADE B REQUIRES A C_{Li} OF 0.626 TO GET AN EFFICIENCY OF 0.800 FOR CONDITION 2, BUT ONLY HAS AN EFFICIENCY OF 0.585 FOR CONDITION 1.

3/31/58 V.E.A.
HSD CURVE NO. F-26318

APPENDIX C

GENERALIZED COMPRESSIBILITY CORRECTION CHART

Included in this appendix is a generalized compressibility correction chart that may be used directly with either Appendix A or Appendix B. It is to be used only with conditions for an unskewed propeller. The chart is self explainable.

GENERALIZED COMPRESSIBILITY CORRECTION CHART

USE ONLY FOR AN UNSKEWED PROPELLER

APPENDIX A

$C_{T\ \text{COMPRESSIBLE}} = C_T \times F_c$

APPENDIX B

$\eta_{\text{COMPRESSIBLE}} = \eta \times F_c$

M_o – FLIGHT FORWARD MACH NUMBER
N – PROPELLER SPEED – RPM
D – PROPELLER DIAMETER – FEET
C_{Li} – INTEGRATED DESIGN C_L
$J = 101.4\, V_K / ND$
f_c = RATIO OF SQUARE ROOT OF ABSOLUTE TEMPERATURE $= \sqrt{T_o/T}$

M_o COMPRESSIBILITY BELOW THIS LINE

$ND \times f_c$

23,000
20,000
18,000
16,000
14,000
12,000
10,000

$M_o = .30$ .35 .40 .45 .50 .55

f_c

.8 1.2 1.6 2.0 2.4 2.8 3.2 3.6

J

$M_o = .30$ .35 .40 .45 .50 .55

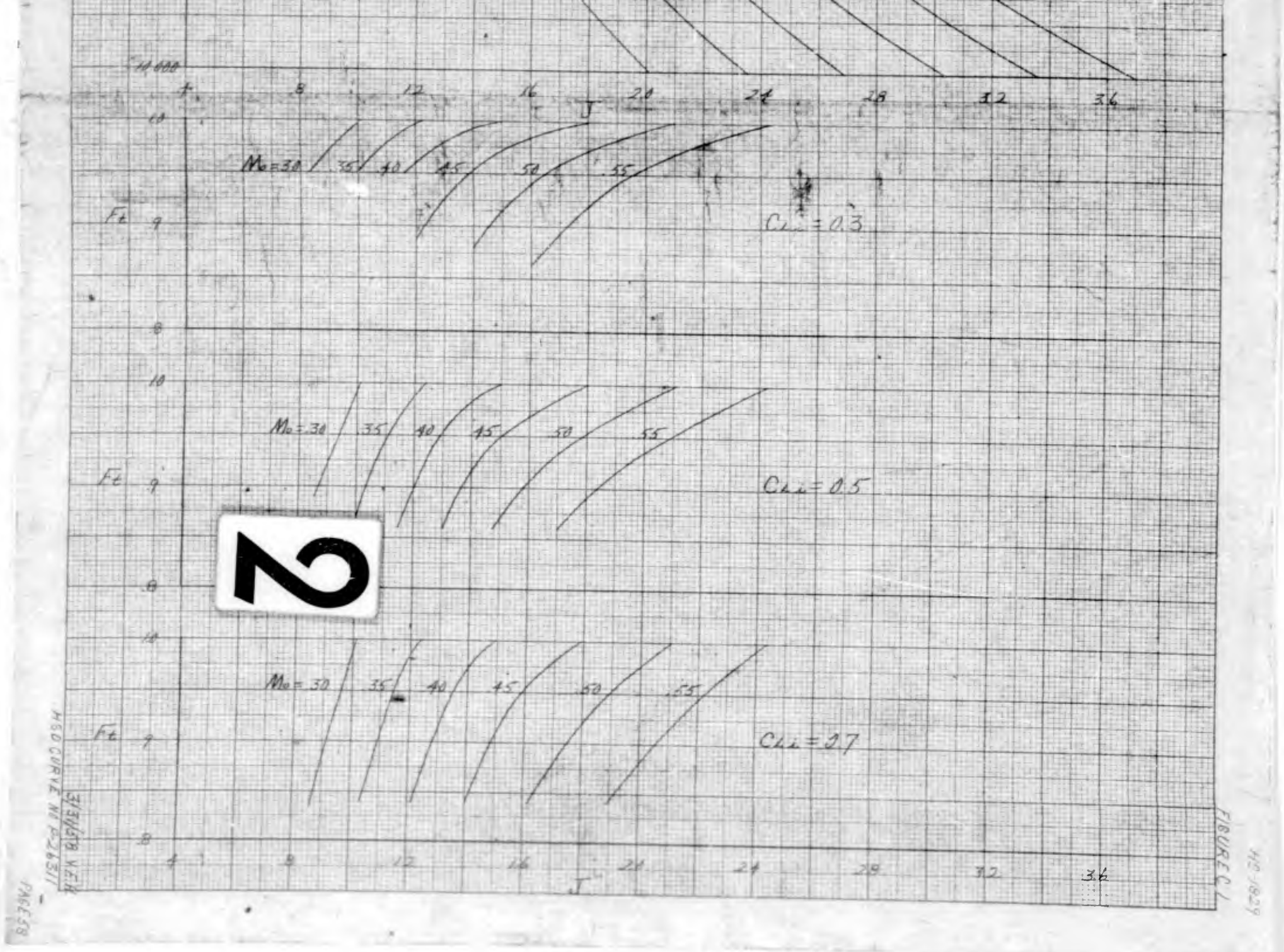

2

HSD CURVE NO. 26311

FIGURE C-1

PAGE 58